Ares Aerospace *presents*
F-57 Man O' War

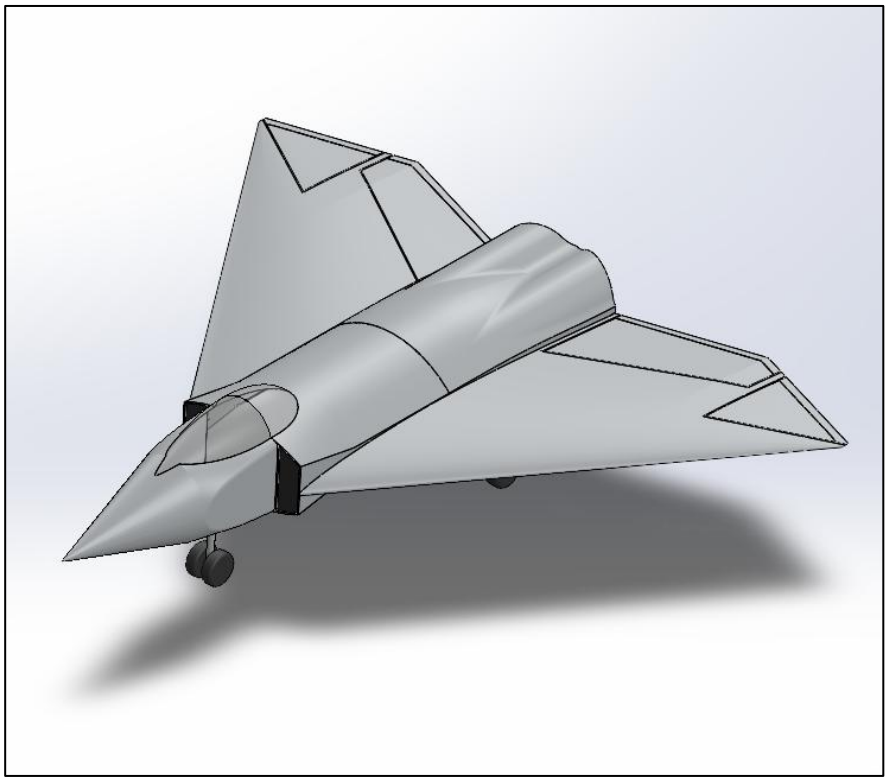

In response to the 2025-2026 AIAA Next Generation Carrier-Based Strike Fighter Aircraft Undergraduate Competition

SDSU | College of Engineering

Presented by San Diego State University

Aerospace Engineering Department

Aircraft Design

Aerospace Engineering Team

Aerospace Engineering Team

Cristian Rosete
Project Manager

Jake Figone
Performance Lead & Consultant

Joaquin Long
Propulsion Lead & Systems Lead

Maxwell Weaver
Aircraft Design and CAD Lead

Shawn Obeso
Structure Lead & Consultant

Table of Contents

List of Figures

List of Tables

Nomenclature

C_p	=	pressure coefficient
Cx	=	force coefficient in the x direction
Cy	=	force coefficient in the y direction
c	=	chord
dt	=	time step
Fx	=	X component of the resultant pressure force acting on the vehicle
Fy	=	Y component of the resultant pressure force acting on the vehicle
f, g	=	generic functions
h	=	height
i	=	time index during navigation
j	=	waypoint index
K	=	trailing-edge (TE) nondimensional angular deflection rate
W_{TO}	=	Take-off Weight
W_{OE}	=	Manufacturers Empty Weight
W_{Fuel}	=	Fuel Weight
W_{PL}	=	Payload Weight
W_{Fixed}	=	Fixed Equipment Weight
W_{Crew}	=	Crew Weight
W_{tfo}	=	Trapped Fuel and Oil Weight
MAC	=	Mean Aerodynamic Chord
V_{stall}	=	Stall Velocity
$V_{approach}$	=	Approach Velocity
$V_{engaging}$	=	Engaging Velocity
V_{stop}	=	Stopping Velocity
V_1	=	Decision Velocity
V_R	=	Rotation Velocity
V_{TO}	=	Take-off Velocity
V_{obs}	=	Obstacle Velocity
V_{EF}	=	Engine Failure Velocity
V_∞	=	Freestream Velocity
M_∞	=	Freestream Mach
a_∞	=	Freestream acceleration
a_{go}	=	Go acceleration
a_{brake}	=	Brake acceleration
$\dot{m}$	=	Mass flow rate
ρ_∞	=	Density
η_{cap}	=	Cap Efficiency
A_{intake}	=	Intake Area
OEI	=	One Engine Inoperable
S_{BFL}	=	Balanced Field Length
s_{brake}	=	Brake Distance
TAC	=	Total Accumulated Cycles
TSFC	=	Thrust-Specific Fuel Consumption
FOD	=	Foreign Object Debris
C_{L_α}	=	Aircraft Lift Curve Slope
β	=	Compressibility Factor
AR	=	Aspect Ratio
Λ	=	Sweep Angle
E	=	Airframe engineering
D	=	Development support cost
F	=	Flight Test Operations
T	=	Tooling
L	=	Manufacturing Labor
QC	=	Quality Control
M	=	Total Cost of Materials
P	=	Engine
$\left(\frac{W}{S}\right)_{TO}$	=	Take Off Wing Load
C_{Do}	=	Induced drag polar coefficient
C_L	=	Lift coefficient
k	=	Parasitic drag polar coefficient
C_D	=	Drag coefficient
C_M	=	Moment coefficient

I. Executive Summary

With the sensitive and unstable state of geopolitics the impending conflicts overseas drive for the United States Navy to act under short notice. Many foreign operations that the United States must deal with are combatting enemies on terrain and in air-to-air combat. With the current evolution of high precision advanced multi-mission system radars such as Lockheed Martin's Sentinel A4 and Northrop Grumman's G/ATOR, the next generation of fighter jets must have sleek features that go against traditional military aircraft. The renovation of the aircrafts body is highly driven to remain undetectable under these high precision tools. Under different mission operations the navy must have a reliable aircraft that will highlight payloads with characteristics such as heat seeking, short range, medium range, air to air, infrared guidance, and multi-mission configurations. The method of storage then comes into play due to the nature of transportation for navy aircraft. The rough sea conditions play a huge role in the erosion of crucial components on the jet. Propulsive systems therefore become a huge nuisance when finding aircraft that are compatible for takeoff on such short distances and conditions due to the sea.

The F-57 Man O' War is a twin-engine, carrier-based multirole aircraft developed as a conceptual and preliminary design study to meet AIAA design requirements for combined air-to-air and air-to-ground missions from U.S. Navy aircraft carriers. The project investigates whether a tailless flying-wing configuration, similar in concept to the B-2 bomber and powered by two GE F110-GE-129 afterburning turbofan engines, can satisfy a 700 nautical mile combat radius, dash and loiter segments, and full day/night carrier operations. Standard aircraft design methods are applied, including constraint analysis, parametric sizing, aerodynamic and weight estimation, mission performance simulation, and carrier suitability assessments. Results indicate that the baseline F-57 configuration can meet the primary mission radius and carrier launch and recovery requirements with acceptable fuel fraction and performance margins. The study concludes that a tailless carrier-based configuration is a viable candidate for future naval strike and air-to-air roles, and it identifies key sensitivities in wing loading, fuel volume, and thrust that inform recommendations for further aerodynamic, structural, and systems refinement.

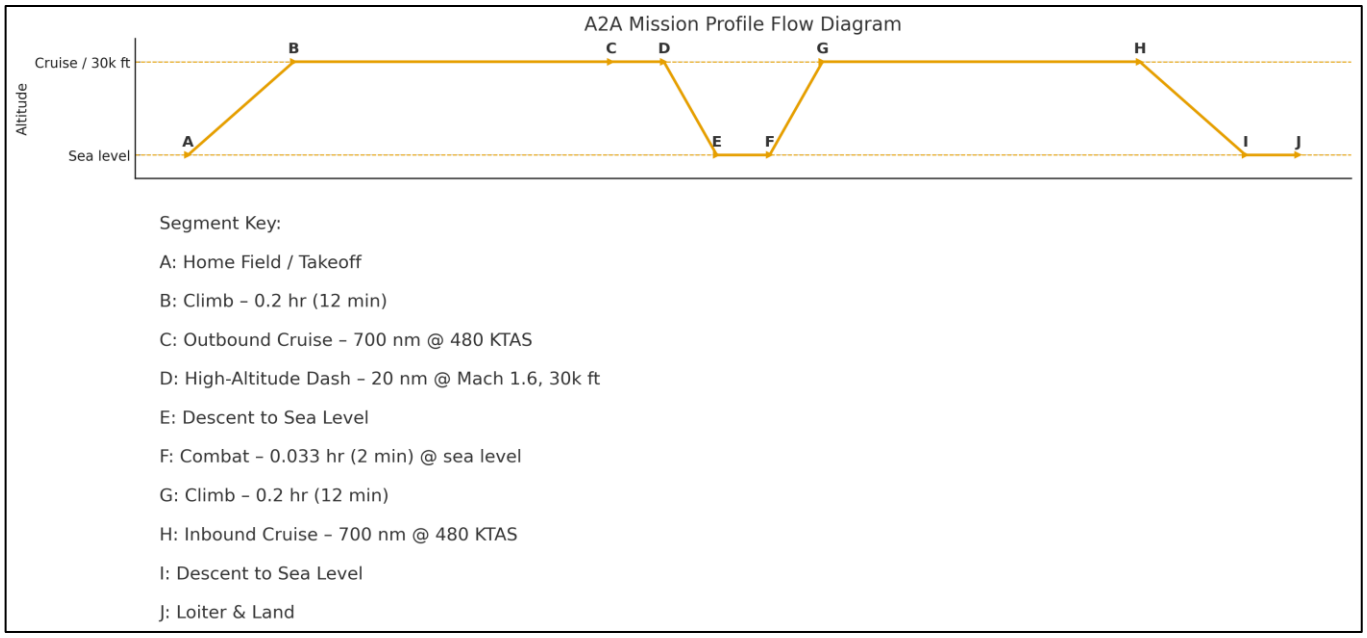

Figure 1: Air to Air Mission

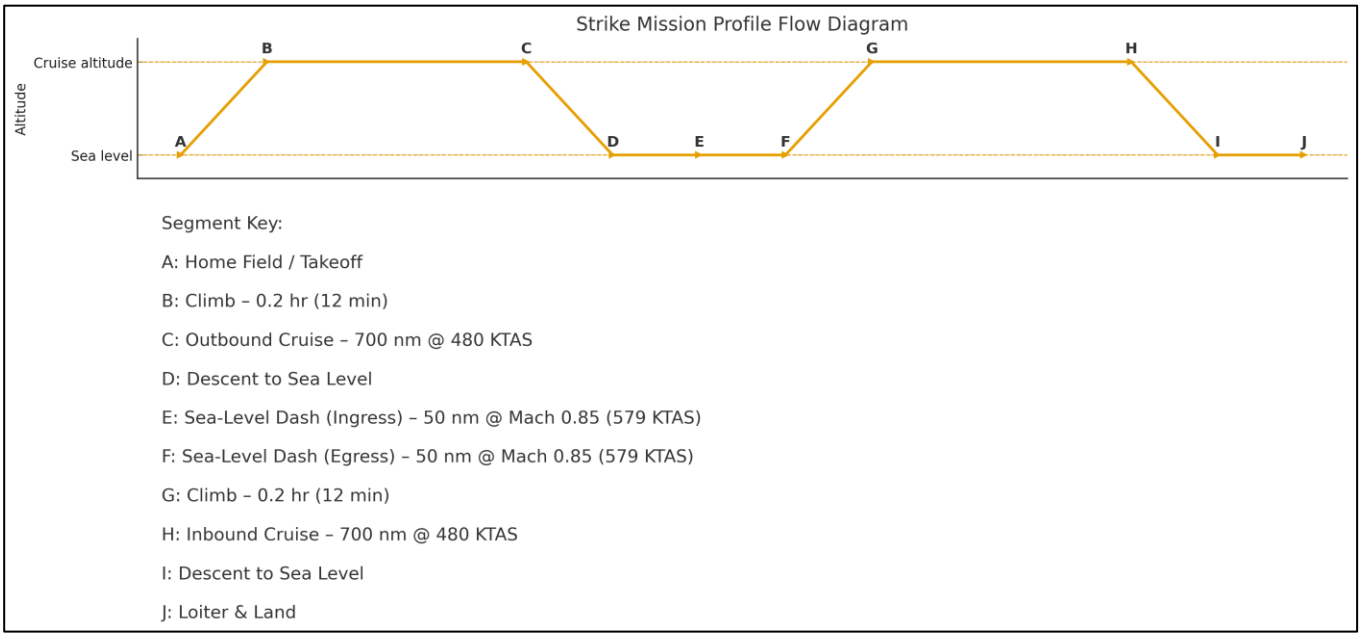

Figure 2: Strike Mission

At the F-57's current state Area Aerospace can achieve the desired configuration that the United State Navy recommended for all navy aircraft. The current design showcases the concept of the plane without traditional vertical stabilizers and for the next iteration of the paper the team shall include CAD models that display the possibility of additional high lift devices and control surfaces at all configurable positions. The document will go over how each set up will affect the maneuverability of the aircraft. The current concept has highlighted the exterior body, although the next iteration will include the drawings of the internal portions of the aircraft. The team will highlight the spars, ribs, webs, fuel tanks, frames, bulkheads, longeron, payload bay, and cockpit configuration.

The next iteration will focus on verifying that the system can takeoff at the provided catapult speed of $69.45\frac{m}{s}$. The current governing airspeed at takeoff in air-to-air is around $71.35\frac{m}{s}$, while the strike configuration demands a velocity of about $72.16\frac{\mathrm{m}}{\mathrm{s}}$. The current discrepancies are $1.9\frac{m}{s}$ and $2.71\frac{m}{s}$ respectively for each mission. The remodeling will focus on obtaining a higher lift coefficient, removal of excessive weight and or increasing the surface area of the wing. The catapult speed that is obtained is derived from the deadload weight of the aircraft and version of carrier the aircraft is being launched from.

The landing gear for the plane is currently under heavy development as the team is trying to innovate the method of retraction. Due to the nature of the wings volume the team has run into issues with trying to find a suitable method of storing the designated landing gear. All current values that are documented mathematically are subject to change as the redesign will incorporate a shift in volume within the wing and the mass value for the aircraft at landing and takeoff weight will differ significantly.

II. System Requirements

The current design for the F-57 was heavily influenced by the request for proposals given out by the American Institute of Aeronautics and Astronautics. The following description was given that the replacement models for the FA-18E/F aircraft must have improved performance at a competitive cost per unit. The major objective for the following proposal is to design a project that encompasses affordability, carrier-based aircraft transportation that can provide credible advanced air defenses and counter air environment.

The major requirements, constraints and guidance for the aircraft are presented as: general design, carrier suitability, launch performance, payload, mission and point performance requirements.

From a high-level perspective the general design has outlined the following sections of configuration, propulsive systems, materials, subsystems, and ordnance carriage. As defined, the aircraft must include any combinations of survivability, vulnerability and effectiveness features to maximize its cost-effective capability. Leading the team to design an aircraft that for the proposed cost would meet the requirements detailed in the AIAA request for proposal. The trade off from price would include key component parts that are easily manufacturable and replaceable with current items being easily accessible on the market. The propulsive systems section requires that the aircraft be a single or multi-engine design, with the engines(s) that are currently existing in productions to minimize the cost of development. The aircraft shall be made of materials that are suitable for a 25-year service life in maritime environments that include moisture, erosion, and salt spray. The plane shall also be made of materials that are currently accessible in the current market to reduce the amount of cost in development. Subsystems are defined as having technologies that are currently at a technological readiness level of 6 or higher. The final section for the general design is ordnance carriage where the aircraft is recommended to have internal carriage of weapons to reduce the cross-radar section.

The next constraint has been outlined as carrier suitability. As defined in this section the aircraft shall be operable from the CVN-68 and CVN-78 class aircraft carriers. The current CVN carriers are equipped with cable arrestment configurations where the kinetic energy is translated to a hydraulic system or electromagnetic motor. The aircraft must have minimal impact on the operation for the carrier air wing. This includes but is not limited to compatibility with preexisting shipboard equipment, and time or crew support required for launch.

Launch performance is outlined as the following for section for constraints. The aircraft must be capable of launching on a tropical day with temperatures at 89.5°F with zero wind over the deck. Therefore, since their aircraft will be launching on a navy vessel the defined air speed required at the end of the catapult stroke must support the aircraft under the conditions of altitude loss, lift limit, pitch rate limit and longitudinal acceleration specified for catapulting. The minimum air speed shall be defined as the highest value obtained from the following calculations: a 90% maximum lift coefficient, an air speed where the aircraft has a longitudinal acceleration of 0.065g at zero flight plan angle, and a minimum aircraft control speed for a one engine inoperative configuration.

Recovery requirements follow as arrestments engaging speed shall be assumed to be 5% greater than approach speed. Next, the approach speed shall be greater than 10% above the stall speed, but less than 145 or about $75\frac{m}{s}$. Finally the arrestment landing weight shall include sufficient fuel for a 20 minute loiter at 10,000 feet with two landing attempts at 25% maximum fuel weight and 50% store weight.

Payload requirements are therefore defined as the air-to-air combat and strike mission configuration. This includes having an avionics suite with a maximum weight of 2,500 pounds located in the internal airframe. The payload ordnance shall be able to store six AIM-120C, two AIM-9X or four MK-83 JDAM missiles. Mission requirements are highlighted in figure 1 and 2 under the executive summary in section 1. Reference table 1-1 for the requirement matrix that have been annotated to display the status version one of the Man O' War. The colors used in the matrix are as follows: blue verifies that the requirement has been met, yellow states that the section values are close to being met, while red signifies not meant. As seen in table 111 above 33/41 requirements are blue, with the remaining 7 yellow and 1 red requirement to be discussed in more detail during their respective sections of this report.

Table 1-1: Requirement Matrix

No.	Navy Cruiser	Required/Desired Values
1	Propulsion Configuration	Single or Multi
2	Engine Type	Existing Engine
3	Design Service Life	Suitable for 25-year maritime environment
4	Subsystems Maturity	TRL≥6(incl. avionics/mission systems)
5	Ordnance Carriage	External acceptable, Internal desirable
6	Carrier Classes	Operable from CVN-68 and CVN-78
7	Fleet Impact	Minimal; compatible with shipboard equipment; minimal time/crew for launch
8	Launch Conditions	89.8 °F tropical day; WOD = 0 kt
9	Catapult end-speed (sink/deck run)	≤10 ft sink; ≤32 ft post-stroke deck run
10	Catapult end-speed (lift limit)	≥ speed at 0.9 CLmax (power-off, OGE)
11	Catapult end-speed (acceleration limit)	≥ speed where ax ≥ 0.065 g at γ = 0°
12	Catapult end-speed (control, multi-engine)	≥ minimum control speed with one engine inoperative
13	Arrestment engaging speed	V_engage = 1.05 × V_approach
14	Approach speed limits	>1.10 × V_stall and <145 kt
15	Arrestment landing weight basis	Include fuel for 20 min loiter @10k ft + 2 landing attempts; 25% max fuel wt; 50% store
16	A2A avionics/sensors	2,500 lb (internal)
17	A2A weapons load	AIM-120C ×6; AIM-9X ×2
18	Strike avionics/sensors	2,500 lb (internal)
19	Strike weapons load	MK-83 JDAM ×4; AIM-9X ×2
20	A2A combat radius	≥700 nm (1,000 nm desirable)
21	A2A max-thrust turn	≥2 min at best-turn speed @10k ft (5 min desirable)
22	A2A stores retention	Carry ordnance for the entire mission (incl. arrestment)
23	A2A sustained turn rate	≥8.0 deg/s @20k ft, mid-mission fuel (10.0 deg/s desirable)
24	High altitude dash	Mach 1.6 @30k ft (Mach 2.0 desirable)
25	Strike combat radius	≥700 nm (1,000 nm desirable)
26	Strike sea-level dash legs	50 nm ingress + 50 nm egress @ intermediate thrust (max non-AB)
27	Strike dash speed (sea level)	Mach ≥0.85 @ intermediate thrust (0.90 desirable)
28	Strike stores retention	Carry ordnance for the entire mission (incl. arrestment)
29	Vertical Load factor	Nz > 7 g @ mid-mission weight (8 g desirable)
30	External store capacity (total)	≥10,000 lb
31	External store capacity (single)	≥3,000 lb
32	Launch system and WOD	C-13-2 catapult; WOD ≤ 0 kt
33	Recovery system and WOD	Mk-7 Mod-3 arresting gear; WOD ≤ 15 kt
34	SEROC at launch (multi engine)	≥200 ft/min
35	SEROC on approach (multi-engine)	≥500 ft/min
36	Unfolded wingspan	≤60 ft
37	Folded wingspan	≤35 ft
38	Overall length	≤50 ft
39	Overall height	≤18.5 ft
40	Stowed spot factor	Minimize total planform area (guidance)
41	Maximum takeoff gross weight	≤90,000 lb

III. Aircraft Description

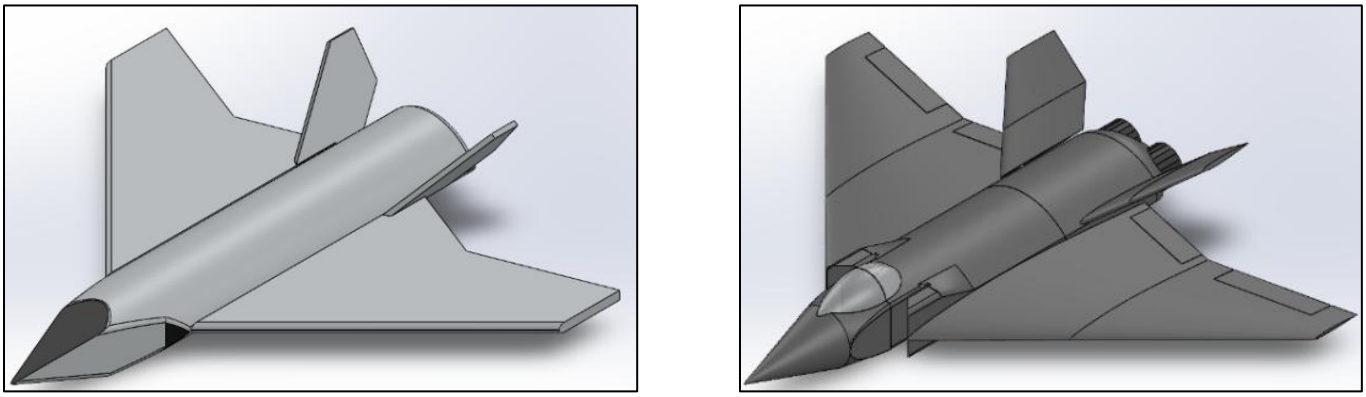

a) *b)*

Figure 3: Preliminary CAD Design a) First Mockup and b) Updated Preliminary Design

3.1 Preliminary Sizing

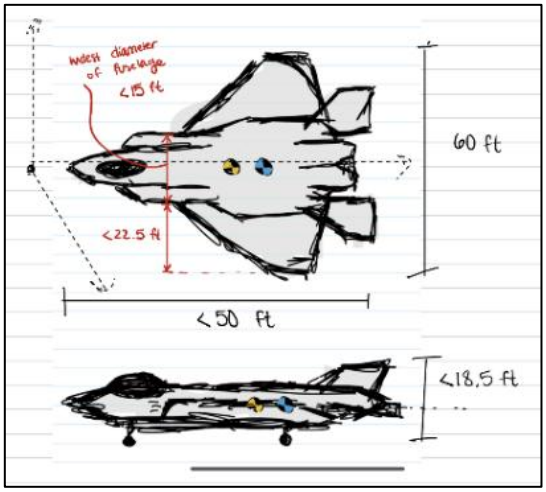

Figure 4: Preliminary Centers of Gravity and Pressure

In the preliminary size of their aircraft, most of the findings were driven by the F/A-18E/F, the F-22, and the F-35C, two of which can be seen below in figure 9 and 10. The team referred to them consistently and essentially found attempting to improve the Super Hornet and implementing bits and pieces of the other two aircraft. Although most of their early sizing is heavily influenced by said aircraft, the team were still conservative in their estimates. For instance, their initial final weight was 67000lb, whereas their max final weight was 56, 203 lb. There were several criteria that required assumptions that the team could not accurately find from what was readily available of modern aircraft, such as the fuel capacity, avionics, and landing gear, but the team was able to get an estimate from what the team could find, which is how the team found their initial operating empty weight to be 40000lb, which eventually dropped by several thousand pounds as the team progressed further into their design. Although their initial estimates were relatively high compared to their final weights, it gave us a rough idea as to what to expect of their aircraft, not only from researching modern aircraft in as much detail as was possible, but also from what the desires of their aircraft, such as an internal weapons bay, thrust vectoring, high maneuverability, and an engine suitable for a carrier.

Figure 5: Recovery of an F/A-18E/F on a carrier

Figure 6: F-35C fueling for mission

Moving on to the takeoff thrust, it is directly related to the engine of choice. The team opted for the F110–GE-129 and considering the team is performing an assisted launch with the catapult, the aircraft will be launched at full afterburner. Therefore, their thrust per engine will be 29,000 lbf, providing a total of 58,000 lbf of takeoff thrust due to their dual engine requirement. However, the velocity the aircraft require for takeoff unfortunately exceeds the velocity the catapult will provide. The solution to this is to use high-lift devices, which will be talked about in a succeeding section. On the topic of lift, the team initially found the surface area of the wings from knowing the desired takeoff velocity, weight, and max lift coefficient. This resulted in wings that were too large due to the larger weight in the beginning of the process. After finalizing the weight, the team found the ideal wing areas to be 662.3 ft^2 per wing. This area provides an aspect ratio of 2.4, and a max wing loading of 84.86 $\frac{lb}{ft^2}$, both of which are ideal for a naval jet prioritizing dash, climb, and combat.

Another crucial component of the aircraft is landing gear. It will consist of a tricycle setup, having two single struts on the main gear with one wheel each, and a single strut on the nose gear with two wheels, which is comparable to both the F/A-18 and the F-35C, seen below in figures 11 and 12. From their CG, the team found the best location for the main gear will be 422in behind the tip of the nose cone – the reference point – and at the intersection between the fuselage and wings because it provides the most structural support. Fully extended they will sit 114in below the tip on the nose cone. For the nose gear, it was calculated that 168in directly behind the reference point would be ideal and fully extended will sit 95in below. The locations provide the total landing load the main will need to withstand, which would be 96, 898.96lb, leading to individual strut loads of 48, 449.48lbs, and due to their single wheel setup, will be the load on the wheel. The nose must withstand a total of 11, 014.63lb, and thanks to the dual wheel setup, each wheel on the strut will split the load capacity, for a total of 5, 507.31lb on each. Lastly, the team found the total reactions to be 85.43% and 14.57%, which are the respective percentages of the total landing loads the main and nose gear will support. With all known information, it allowed us to finalize the tires: the main gear tires will be bias-ply tires rated for ≥ 50000 lb per wheel at 320psi, have a 14in tire width, and a diameter of 34in; the nose gear will be rated for ≥ 6000lb per wheel at 260psi, a 10in width, and a 28in diameter.

Figure 7: Showcase of F/A-18 Landing Gear

Figure 8: F-35C Landing Gear

3.2 Preliminary Configuration

The cockpit of the F-57 Man-O'-War has a cockpit of 198 inches in length, and a maximum height of 90 inches, to functionally fit a single pilot and their necessary instruments. Sitting directly behind the cockpit will be a dual set of air intakes on each side as well as the leading edge of the swept wings.

The Airfoils chosen for the wings are NACA 64A-206. This airfoil was chosen for its low drag characteristics at subsonic and transonic speeds. This allows for higher cruise efficiency and larger combat radius, which is critical for a carrier-based aircraft that must fly farther with less fuel. This airfoil has a favorable pressure distribution for high swept wings that are also employed in this aircraft due to its 6% thickness. This thickness also allows for an optimization in low wave drag and stealth geometry. This airfoil is known to have a smooth pitching moment curve which would be optimal for the tailless fly-by-wire heavy design. The NACA 600 series is a tried and well documented series of airfoils, and its verified and effective characteristics complement their design philosophies.

The wings are placed 198 inches aft of the tip of the cockpit, as the aircraft must be relatively compact for storage on aircraft carriers. To create a geometrically sound wing, an important core in the verification of the viability of further aircraft attributes, a planform of the wing was created using Microsoft Excel. A leading-edge sweep of 55 degrees was chosen to maximize stealth geometry as well as supersonic efficiency. To continue the supersonically optimized geometry down the span of the wing, a taper is required. As the maximum total span of the aircraft is 60 feet, the half span of the wing was designed to be well under, reaching 240 inches, or 20 feet. Since the wings would also have to fold during storage, a minimal amount of the wing would be required to fold using a smaller size of the total span. To maximize wing area, the wing extends back to 588.151 inches from the tip of the most forward point of the aircraft. This satisfies the requirement that the total length of the aircraft is no longer than 600 inches. The wing tapers twice, to follow stealth geometry. Halfway down the half span, the root chord length goes from 350 inches to 218.8 inches giving a taper ratio of 0.625. The second taper goes from this point, the halfway point down the half span, to the tip. The tip chord length is only 7.2 inches, so the second taper ratio is 0.033. The total average taper ratio is 0.02. The trailing edge is also given a sweep of 18.5 degrees and changes directions at the point of the changing tapers to give the aircraft a reduced radar signature. A single wing has an aspect ratio of 2.4, and a total surface area of 662.3 ft², which are within the targets of the aerodynamic capabilities to be further discussed. The Planform generated is provided in the following figure.

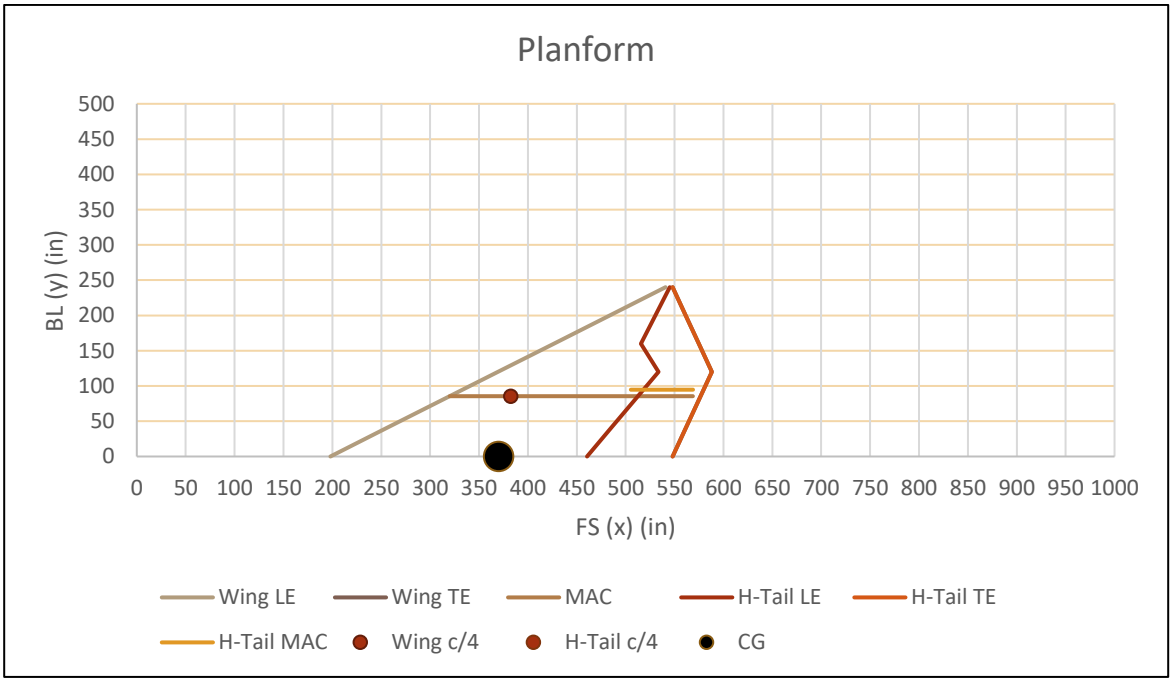

Figure 9: A Planform of the wing created for the aircraft

The control surfaces used in the aircraft are visible in the planform as the geometry on the trailing edge. As there is no empennage on this aircraft, the control surfaces must do all the work for pitch, roll, and yaw authority. The wing has two different types of control surfaces. The inward control surfaces, which extend from the wing root to 139 inches, with a total surface area of 118.5 ft². These are the elevons, which are used exclusively for pitching and rolling the aircraft. They are split, meaning they deflect the air above and below the wing for more control authority that would be necessary without a tail. The other control surface is the split-rudder, which has a span of 96.98 inches and a singular surface area of 66.2 ft². The split-rudder will extend during flight to induce a drag, creating a yawing moment. The deflection angles of the control surfaces can be fine-tuned to the necessary authority required for stable flight. An image of a rendering of the wing with these surfaces included is provided in the following figure

.

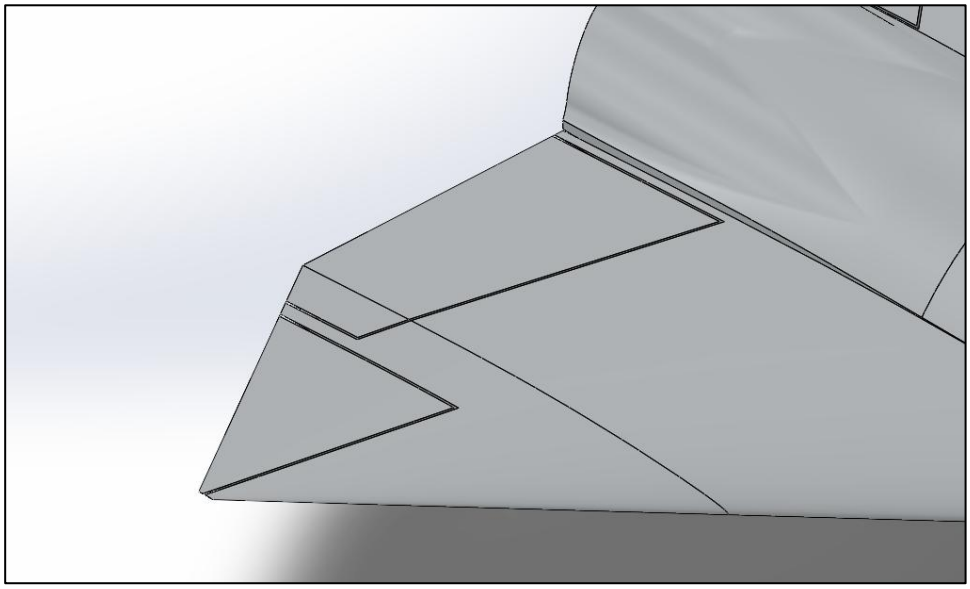

Figure 10: The elevon (larger) and the split-rudder (smaller) control surfaces.

The engines used in the aircraft are the F110–GE–129. A proven naval aircraft engine, with its validity and specifications explained further in this paper. With a length of 182 inches, they are located the most aft of the aircraft, with the engine bay extending 569.94 inches from the front of the aircraft. This is constraint by keeping the overall aircraft flush with the leading edge of the wing. This geometry gives the total engine bay section of the aircraft to be 205 inches, giving ample room for both engines as well as any necessary mechanical parts. The remainder of the body of the aircraft will be used for payload and other fuel storage that may need to be pumped or stored out of the wings. This allows 169-inch-long payload and service bay to sit between the cockpit and the engine bay. With a fuselage diameter of 10 feet, the necessary payload required should be able to fit snugly into the payload bay.

For the landing gear, a tricycle set up design was selected, a pair aft of the center of gravity and a dual wheel landing gear near the nose cone. The forward landing gear will sit in the nosecone section 168 inches from the tip and extend 95 inches from the bodyline of the aircraft. This landing gear will support 14.57% of the aircraft's weight equating to approximately 11,000 pounds. The other two landing gears will sit symmetrically of each other, 422 inches from the front of the aircraft attached to the engine bay, they will be offset by 114 inches away from the centerline of the aircraft and will support 85.43% of the aircraft's weight equal to 48,500 pounds. This geometry ensures the center of gravity lies well in between the landing gear allowing for safe and balanced landings to be performed on an aircraft carrier.

3.3 Configuration and Drawings

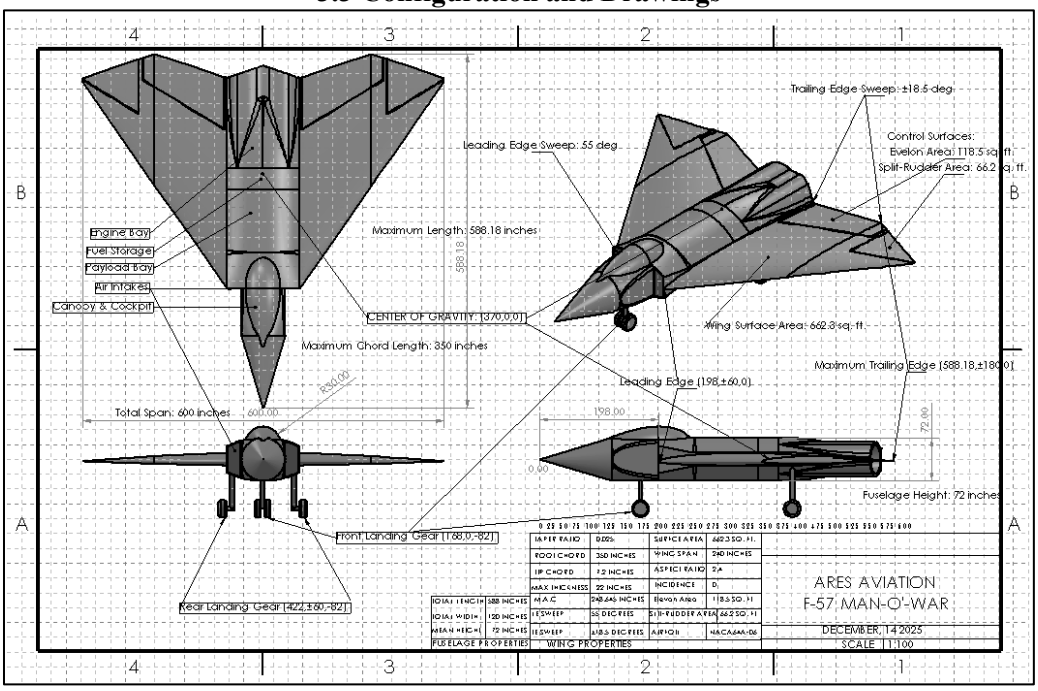

Figure 11: General Arrangement 3-View Drawing

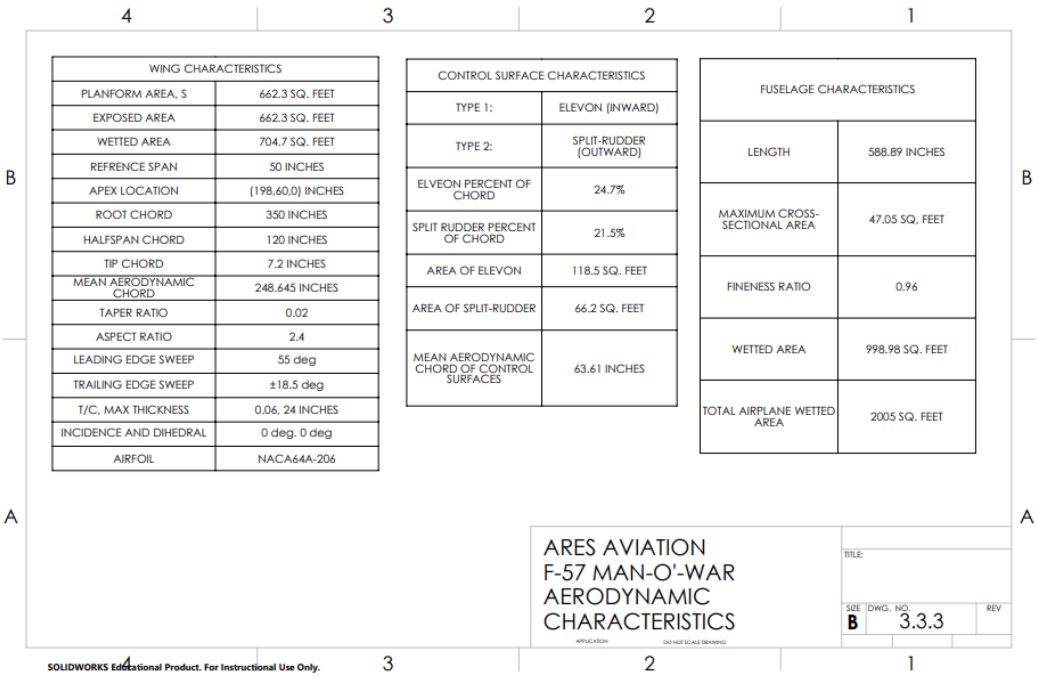

WING CHARACTERISTICS	
PLANFORM AREA, S	662.3 SQ. FEET
EXPOSED AREA	662.3 SQ. FEET
WETTED AREA	704.7 SQ. FEET
REFRENCE SPAN	50 INCHES
APEX LOCATION	(198,60,0) INCHES
ROOT CHORD	350 INCHES
HALFSPAN CHORD	120 INCHES
TIP CHORD	7.2 INCHES
MEAN AERODYNAMIC CHORD	248.645 INCHES
TAPER RATIO	0.02
ASPECT RATIO	2.4
LEADING EDGE SWEEP	55 deg
TRAILING EDGE SWEEP	±18.5 deg
T/C, MAX THICKNESS	0.06, 24 INCHES
INCIDENCE AND DIHEDRAL	0 deg, 0 deg
AIRFOIL	NACA64A-206

CONTROL SURFACE CHARACTERISTICS	
TYPE 1:	ELEVON (INWARD)
TYPE 2:	SPLIT-RUDDER (OUTWARD)
ELVEON PERCENT OF CHORD	24.7%
SPLIT RUDDER PERCENT OF CHORD	21.5%
AREA OF ELEVON	118.5 SQ. FEET
AREA OF SPLIT-RUDDER	66.2 SQ. FEET
MEAN AERODYNAMIC CHORD OF CONTROL SURFACES	63.61 INCHES

FUSELAGE CHARACTERISTICS	
LENGTH	588.89 INCHES
MAXIMUM CROSS-SECTIONAL AREA	47.05 SQ. FEET
FINENESS RATIO	0.96
WETTED AREA	998.98 SQ. FEET
TOTAL AIRPLANE WETTED AREA	2005 SQ. FEET

3.3.2: Drawing Table

3.3.3: Inboard Profile: TBD

IV. Mass Properties

In this section, the team calculated the mass-properties model of the F-57 Man o' War and its role in enabling a credible overall aircraft design. A mass properties spreadsheet is first developed using standard empirical methods, leading to summary tables of empty weight, fuel, payload, crew, and key operating weight conditions for the missions specified in the system requirements document. Component weights and their locations are then tabulated in the aircraft coordinate system, allowing calculation of center-of-gravity positions for all required loading cases and configurations. The resulting CG travel is expressed in both fuselage station and percent means aerodynamic chord to demonstrate that the CG remains within acceptable limits over the mission envelope. Together, these results provide the foundation for subsequent performance, stability and control, structural sizing, and carrier-suitability analyses, ensuring that all aerodynamic and propulsion estimates are tied to a realistic and consistent mass model.

4.1 Detailed Weight Estimate

The gross takeoff weight calculation is inherently an iterative process because of the fuel mass ratios $\left(\frac{W_E}{W_{TO}}\right)$ is dependent on their W_{TO} itself. Shown below is both the summation and iterative sizing equations to calculate the same W_{TO}.

Weight Summation Equation:

$$\mathbf{W_{TO} = W_{OE} + W_{Fuel} + W_{PL}}$$

Iterative Sizing Equation**:**

$$W_{TO} = \frac{W_{Fixed}}{1 - \left(\frac{W_{OE}}{W_{TO}}\right) - \left(\frac{W_F}{W_{TO}}\right)}$$

A vital step in solving for the takeoff weight W_{TO} is solving for the Operating Empty Weight (W_{OE}) which is formally defined as the manufacturer's empty weight (W_E) plus the weight of the flight crew, undependable fluids like trapped fuel and oil, and fixed equipment such as APU, furnishing, and air conditioning. Which the team calculated as 29,600 lb.

$$\mathbf{W_{OE} = W_E + W_{crew} + W_{Fixed}}$$

Table 2: Empty Weight Values

Item	Weight (lbs)
Total Skin	2383.3
Window	87
Sparing	1000
Ribs	800
Stringers	600
2 * General Electric F110-GE-129	7840.0
Level 6 Avionics Suite	2500
Landing Gear	3500
Total Sum	18785
Uknown Weight Factor	1.3
Total Empty Weight w/ Unknow Weight Factor	24420

Though this also includes another huge component of mass, which is defined as manufacturer's empty weight (W_E). In this it includes structures, such as fuselage, engines, and landing gear. Shown below is a component-based mass and location table that gives definition to main components their masses, and where they're located in relation to the nose of the plane (0,0,0). The empty weight of the aircraft can be defined as the weight of its structure, engines and all permanently installed equipment. This value would exclude the weight of the crew and any undergoing dynamic changes that are affected during the execution of the mission. The value for the total skin was obtained from the current SolidWorks CAD model. All other values were located on manufacturer specifications sheets. The total

weight for the aircraft came to be about 19,000 pounds. With more research the team found that current weight for a similar model of aircraft at an empty weight comes out be around 29,000 pounds, a difference of about 10,000 pounds. Therefore, the team decided to multiple the total weight calculated by an unknown weight factor of 1.3. This brings their current to about 25,000 pounds. A value that closely resembles the F35-C. The team will determine a more refined value for the empty weight once all internal airframe structures have been added onto the CAD file.

Moving on to another component of mass is the fuel weight (W_{Fuel}). The core of fuel weight is calculating the fuel burn for each mission segment. This is done by finding the weight ratio $\left(\frac{W_{end}}{W_{start}}\right)$ for each segment.

Total mission weight ratio is the product of the individual segment ratios given as:

$$\frac{W_{Final}}{W_{Initial}} = \frac{W_{landing}}{W_{takeoff}} = \left(\frac{W_1}{W_0} \cdot \frac{W_2}{W_1} \cdot \ldots \cdot \frac{W_{Final}}{W_{n-1}}\right)$$

The total mission fuel weight fraction is then:

$$\frac{W_{F,mission}}{W_{TO}} = 1 - \frac{W_{Final}}{W_{TO}}$$

The weight ratio for constant velocity segments is determined by the Breguet equations, which is different based on the type of propulsion. In the case of their aircraft, the team used the jet equations mentioned in Roskam V. Main contributors to end weight depending on the different mission segments such as Taxi/Takeoff which result in .990 ratio while cruising for 700nm result in a ratio of 1.153. Using the Breguet equations results in acquiring an approximate fuel weight. For the strike mission 23,248 lbs and for the Air-to-Air 21,973 lbs.

$$\frac{W_{end}}{W_{start}} = \exp\left[\frac{-R \cdot C}{V \cdot (L/D)}\right] \quad \text{(Range, Cruise)}$$

$$\frac{W_{end}}{W_{start}} = \exp\left[\frac{-E \cdot C}{(L/D)}\right] \quad \text{(Endurance, Loiter)}$$

Table 3-1: Air-to-Air Weight Summary

	Weight (lb)
Operating Empty Weight (W_{OE})	29600
Empty Weight (W_E)	29100
Trapped Fuel and Oil (W_{tfo})	300
Crew Weight (W_{CREW})	200
Fuel (W_F)	21973
W_{OE} + 60% fuel	42784
$W_{OE} + W_F$	51573
Payload Weight (W_{PL})	2508
$W_{OE} + W_F + W_{PL}$	54081

Table 3-2: Strike Weight Summary

	Weight (lb)
Operating Empty Weight (W_{OE})	29600
Empty Weight (W_E)	29100
Trapped Fuel and Oil (W_{tfo})	300

Crew Weight (W_{CREW})	200
Fuel (W_F)	23248
W_{OE} + 60% fuel	43549
W_{OE} + W_F	52848
Payload Weight (W_{PL})	4808
W_{OE} + W_F + W_{PL}	57656

The above tables highlight the results of applying the previous equations. The main differences between the Air-to-Air and Strike weights are the payload and fuel weights. Strike requiring two AIM-9X missiles and four MK-83 JDAM bombs. Air-to-Air requiring six AIM-120C and two AIM-9X. The mission segments being more fuel demanding for strike as seen in Figures 1 and 2. The strike mission requiring more fuel that is placed in the fuselage.

4.2 Weights and CG

Table 4: Air-to-Air Mass Properties

Air to Air Mass Properties					
Item	**Name**	**Weight**	**Distance**		
		W	**X**	**Y**	**Z**
		lb	in	in	in
1	Nose Cone (Skin, Fixed EQ., Window)	8235.5	46.68	0.00	5.11
2	Main Fuselage (Skin)	579.8	294.44	0.00	0.00
3	Engine Bay (2 engines + Skin)	10816	507.40	0.00	0.00
4	Left Wing (Skin, Spars, Ribs, & Stringer)	2444	398.00	-67.49	2.49
5	Right Wing (Skin, Spars, Ribs, & Stringers)	2444	398.00	67.49	2.49
6	Left Wing Fuel	10437	408.00	-57.49	2.49
7	Right Wing Fuel	10437	408.00	57.49	2.49
8	Fuselage Fuel	1100	410.00	0.00	0.00
9	Payload (Internal)	2508	294.44	0.00	0.00
10	Trapped Fuel/Oil	300	294.44	0.00	0.00
11	Pilot	200	65.34	0.00	0.00
12	Nose Landing Gear	700	75.00	0.00	0.00
13	Left Wing Landing Gear	1400	330.00	-47.49	0.00
14	Right Wing Landing Gear	1400	330.00	47.49	0.00
	Σ W	**54,081**	lb		

X_{CG}	Y_{CG}	Z_{CG}
in	in	in
354.190	**0**	**2.004**
%MAC		
4.29%		

Table 5: Strike Mass Properties

Strike Mass Properties					
		Weight	**Distance**		
		W	**X**	**Y**	**Z**
Item	**Name**	lb	in	in	in
1	Nose Cone (Skin, Fixed EQ., Window)	8235.5	46.68	0.00	5.11
2	Main Fuselage (Skin)	579.8	294.44	0.00	0.00
3	Engine Bay (2 engines + Skin)	10816	507.40	0.00	0.00
4	Left Wing (Skin, Spars, Ribs, & Stringer)	2444	398.00	-67.49	2.49
5	Right Wing (Skin, Spars, Ribs, & Stringers)	2444	398.00	67.49	2.49
6	Left Wing Fuel	10437	408.00	-57.49	2.49
7	Right Wing Fuel	10437	408.00	57.49	2.49
8	Fuselage Fuel	2374	410.00	0.00	0.00
9	Payload (Internal)	4436	294.44	0.00	0.00
10	Trapped Fuel/Oil	300	294.44	0.00	0.00
11	Pilot	200	65.34	0.00	0.00
12	Nose Landing Gear	700	75.00	0.00	0.00
13	Left Wing Landing Gear	1400	330.00	-47.49	0.00
14	Right Wing Landing Gear	1400	330.00	47.49	0.00
	Σ W	**57,656**	lb		

X_{CG}	Y_{CG}	Z_{CG}
in	in	in
353.406	**0**	**1.890**
%MAC		
3.33%		

The mass properties of their aircraft encompass weight and their center of gravity. These serve as the foundational dataset for their entire design. While weight determines performance capabilities like range and payload, the distribution of that mass dictates the aircraft's stability and control. For their project the team used the unified Aircraft Coordinate System using Frame Station (FS), Butt Line (BL), and Water Line (WL) coordinates. This standardization is vital because it allows for the precise integration of their different components. Highlighted the team can see the main differences between the Air-to-Air and Strike configuration, the latter requiring more fuel placed in the fuselage and as mentioned above a heavier payload. For the data the team broke down the plane into 14 different segments and utilized CAD software to get accurate CG locations for those segments.

4.3 Longitudinal CG Travel

Table 6: Strike CG Travel

Payload	Gear	%Fuel	FS (in)	%MAC
Full Payload	Up	1	(296.713, 0, 1.387)	-6.45%
		60	(311.931, 0, 1.485)	0.30%
		100	(318.764, 0, 1.53)	3.33%
	Down	1	*In progress*	*IP*
		60	*In progress*	*IP*
		100	*In progress*	*IP*
No Payload	Up	1	(296.964, 0, 1.540)	-6.34%
		60	(313.369, 0, 1.607)	0.94%
		100	(320.47, 0, 1.637)	4.09%
	Down	1	*In progress*	*IP*
		60	*In progress*	*IP*
		100	*In progress*	*IP*

Table 7: Air to Air CG Travel

Payload	Gear	%Fuel	FS (in)	%MAC
Full Payload	Up	1	(296.770, 0, 1.450)	-6.423
		60	(313.501, 0, 1.591)	0.998
		100	(320.944, 0, 1.643)	4.300
	Down	1	*In progress*	*IP*
		60	*In progress*	*IP*
		100	*In progress*	*IP*
No Payload	Up	1	(296.916, 0, 1.540)	-6.358
		60	(314.412, 0, 1.668)	1.402
		100	(322.276, 0, 1,725)	4.891
	Down	1	*In progress*	*IP*
		60	*In progress*	*IP*
		100	*In progress*	*IP*

The tables above summarize the CG locations of the F-57 Man o' War for representative fuel states with both full and zero payload, gear up. With full payload and gear up, the CG moves from FS ~ 296.8 in (-6.4% MAC) at near-empty fuel to FS ~320.9 in (4.3% MAC) at full fuel. For the no-payload case, the same trend is observed: the CG shifts from FS ~ 296.9 in (-6.4% MAC) to FS ~ 322.3 in (4.9% MAC) at full fuel. Interpreted over the mission, this means fuel burn will drive the CG forward by roughly 10-11% MAC, while changes in payload primarily produce a small aft

shift of about 0.4-0.6% MAC at a given fuel fraction. The lateral and vertical coordinates remain essentially zero and near the reference waterline, confirming that the mass distribution is symmetric about the aircraft centerline and close to the intended design reference.

Overall, the current mass model produces a gear-up CG envelope spanning roughly -6% to +5% MAC across the loading conditions considered. This band is moderate and shows the team that payload release has a relatively minor influence on CG location compared to fuel burn, which is favorable for handling and trim as stores are expanded. These preliminary results suggest that the F-57 Man o' War can be trimmed and controlled throughout its mission without excessive pitch-control or trim-drag penalties. Gear-down cases are still in progress and will be used to confirm that approach and landing configurations also remain within the allowable.

4.4 Moments of Inertia

TBD

V. Flight Loads

TBD

VI. Structures

TBD

VII. Lift, Drag and Moment Estimation

7.1 Airfoil C_L vs. α Curves

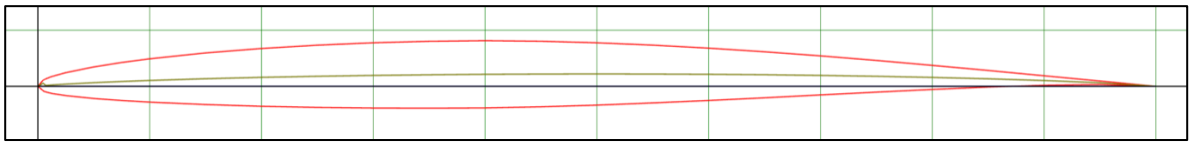

Figure 12: NACA 64-206 Airfoil

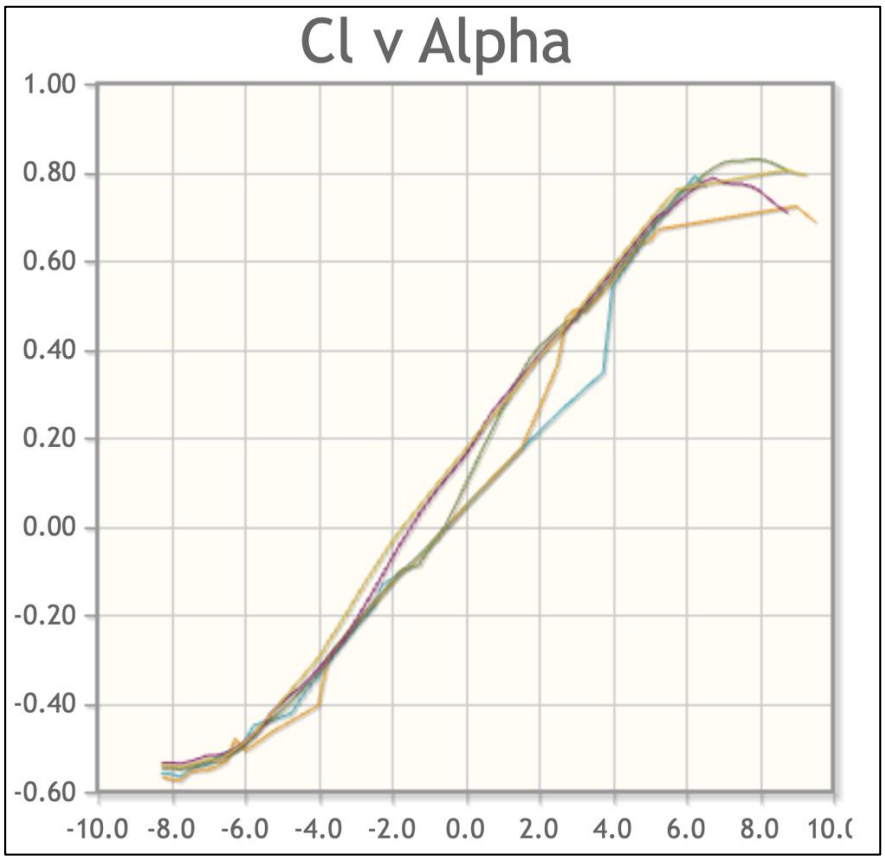

Figure 13: 2D Airfoil Lift Curve

7.2 Lift Curves

The aircraft lift curves are generated at reference conditions of 100 knots at sea level using a temperature of 89.9°F and an air density of $0.002237 \frac{\text{slugs}}{ft^3}$. The Reynolds number was calculated using the wing MAC. Curves were developed for cleaning (CC), takeoff (WTO), and landing (WL) configurations. The F-57 wing is a highly swept 55° delta wing with an aspect ratio of 2.4 and utilizes the NACA 64A-206 airfoil. For both takeoff and landing configurations, symmetric elevon deflection is assumed for lift augmentation. Two-dimensional airfoil analysis seen in the above curve predict that stall of the chosen airfoil to occur around 8°. However, this should be referred to as a section-level characteristic only and not accurate to represent entire aircraft stall. For this type of wing, three-dimensional flow effects come into play when the aircraft reaches elevated angles of attack. Particularly, vortex formation allows the F-57 to operate beyond the two-dimensional airfoil stall angle.

Regarding the specifics of constructing these curves, both linear attached-flow theory and vortex-lift augmentation is utilized. At lower angles of attack, lift was modeled using finite-wing lift-curve theory with aspect ratio and sweep corrections considered. The aircraft lift-curve slope was estimated as:

$$C_{L_\alpha} = \frac{2\pi AR}{2 + \sqrt{4 + \left(\frac{AR\beta}{\cos\Lambda}\right)^2}}$$

Lift augmentation caused by elevon deployment for the WTO and WL configurations was modeled as a constant increment in lift coefficient, reflecting their use as camber-changing surfaces on the F-57's delta wing. For takeoff, an assumed $\Delta C_L = +0.20$ is used, while for landing $\Delta C_L = +0.35$.

At elevated angles of attack with carrier approach and landing, linear attached-flow theory deems itself insufficient for the highly swept delta wing. Beyond the 2D airfoil stall angle, lift is assumed to be dominated by leading-edge vortex formation. This delays aircraft stall, allowing the F-57 to continue generating lift. Accordingly, vortex-lift contribution is included for the WL configuration, where high angle-of-attack operation is expected. Specifically, it is only applied beyond 12°, to reflect the onset of vortex formation on the wing. This value is chosen using the assumption that the transition occurs at $\alpha \approx 1.5 \times \alpha_{airfoil\ stall}$. Vortices strengthen nonlinearly, which can be seen in the behavior of the below curve during this regime.

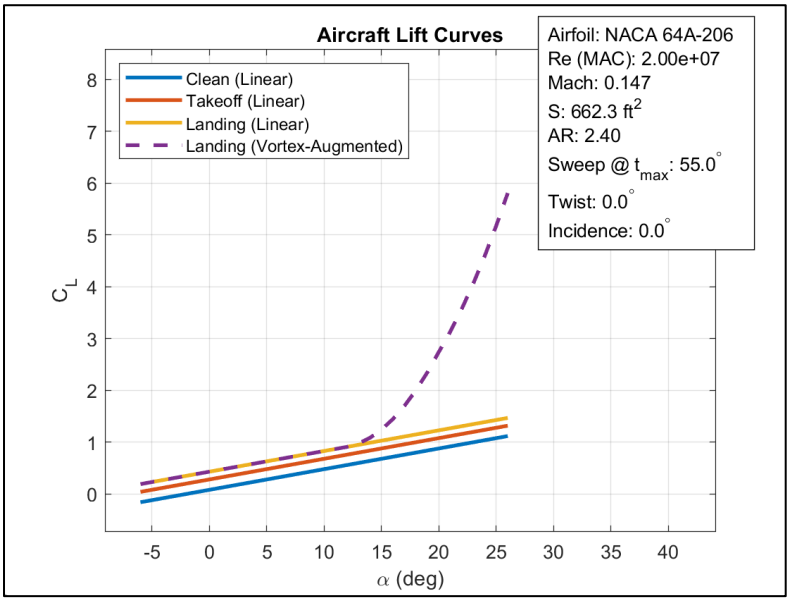

Figure 14: Aircraft C_L vs. α

7.3 Flight Condition Lift Curves

The following lift curves were generated for two mission-specific flight conditions to aid in performance analysis. The first corresponds to a Mach 1.6 air-to-air dash at 30,000 ft. While the second is a Mach 0.85 strike dash at sea level. Clean aircraft configuration was analyzed for both cases, with only the linear attached-flow portion of the curve being considered since high angle-of-attack operation is not considered.

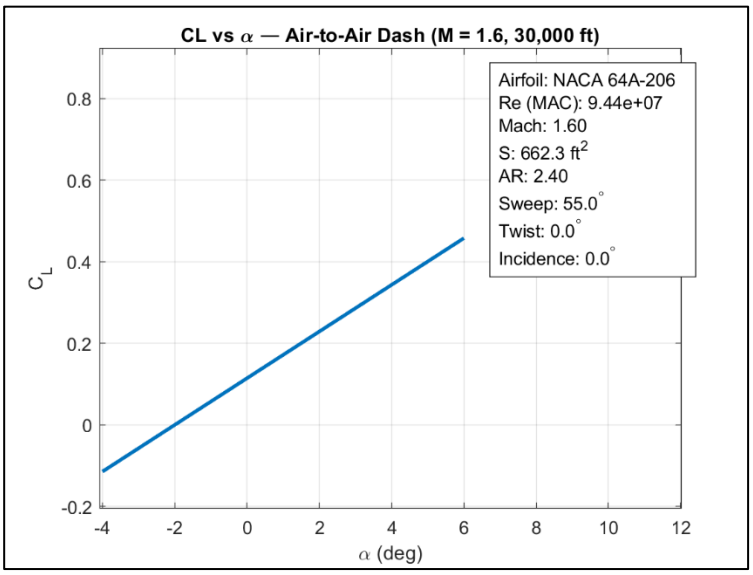

Figure 15: Air-to-Air Dash C_L vs. α

Figure 16: Strike Dash C_L vs. α

7.4 Zero Lift Drag Coefficient

TBD

7.5 Drag Due to Lift Factor (K, K', K'')

TBD

7.6 Drag Polar

This section presents the drag polars for the major configurations used throughout the aircraft's operating envelope. Drag characteristics are shown for the clean configuration, the takeoff and landing states, and all other

configurations required by the mission specification. Because the aircraft employs full internal carriage of all stores, its external aerodynamic shape remains unchanged across combat and cruise conditions, allowing the clean configuration to serve as the baseline for several mission modes. Additional configurations involving high-lift devices and landing gear are included to represent the low-speed phases of operation where drag increases substantially. These drag polars form the foundation for subsequent performance calculations, including takeoff distance, landing approach behavior, climb capability, and high-speed flight assessment.

Figure 17 shows the drag polars for the clean configuration across Mach numbers from 0.70 to 0.95. In this configuration the aircraft carries no external stores and maintains its lowest-drag aerodynamic shape, which makes it the reference condition for cruise, climb, and combat maneuvering. The curves illustrate the gradual increase in drag at higher Mach numbers due to compressibility and the onset of transonic effects. Because all weapons and pylons are housed internally, the clean configuration fully represents the external aerodynamics of the aircraft during normal flight. The drag polar is modeled using a standard parabolic relation:

$$C_D = C_{D0}(M) + kC_L^2$$

where the induced drag factor is $k = 0.1429$. based on the aircraft wing ratio and average Oswald efficiency. The zero-lift drag coefficient C_{D0} is varied with Mach number to represent compressibility and transonic drag rise effects from $M = 0.7$ to $M = 0.95$. As Mach increases, $C_{D0}(M)$ increases, producing the small upward shift in each successive curve. These clean-configuration polars form the basis for all other mission configurations because the aircraft geometry does not change externally (internal weapons carriage), meaning only control surface, gear, or landing-specific increments are applied in later sections.

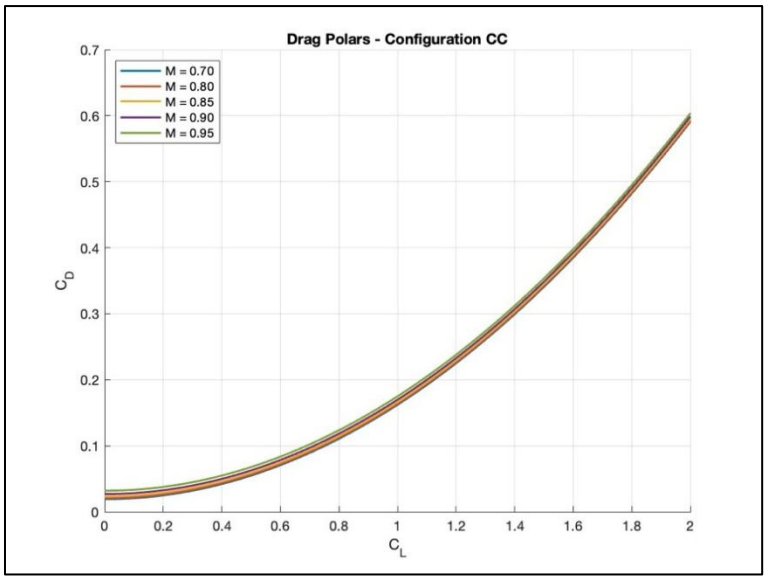

Figure 17: Drag polars for CC (clean configuration)

Figure 17 presents the drag polars for the takeoff configuration at 100 knots indicated air speed and sea-level, hot-day conditions (90F). During takeoff the aircraft operates with takeoff control-surface configuration, and both gear-up and gear-down states are shown to capture the range of drag levels encountered prior to rotation. The increased drag relative to the clean configuration reflects the additional resistance created by high-lift devices and the exposed landing gear. These curves characterize the aircraft in its highest-drag, low-speed regime during the ground roll and initial liftoff.

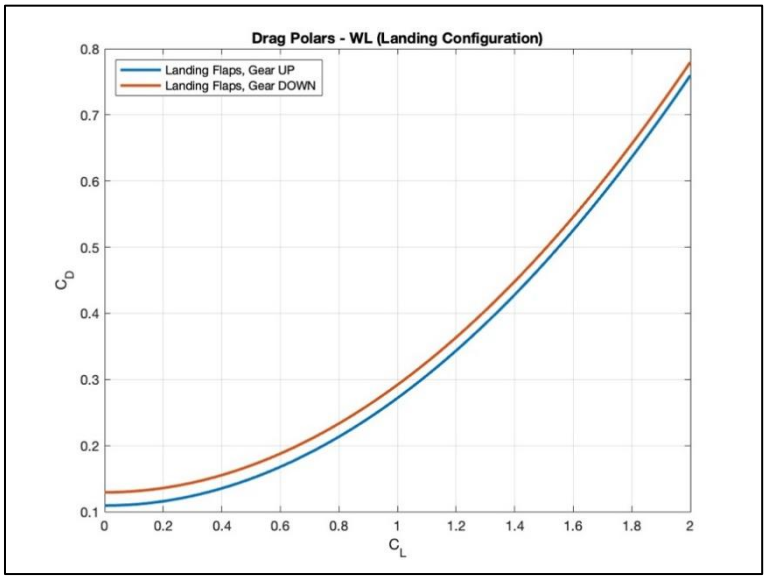

Figure 18: Drag polars for Configuration WL (landing configuration)

Figure 18 presents the drag polars for the takeoff configuration at 100 knots indicated air speed and sea-level, hot-day conditions. During takeoff the aircraft operates with takeoff control-surface deflection, and both gear-up and gear-down states are shown to capture the range of drag levels encountered prior to rotation. The increased drag relative to the clean configuration reflects the additional resistance created by higher-lift configuration and the exposed landing gear. These curves characterize the aircraft in its highest-drag, low-speed regime during the ground roll and initial liftoff.

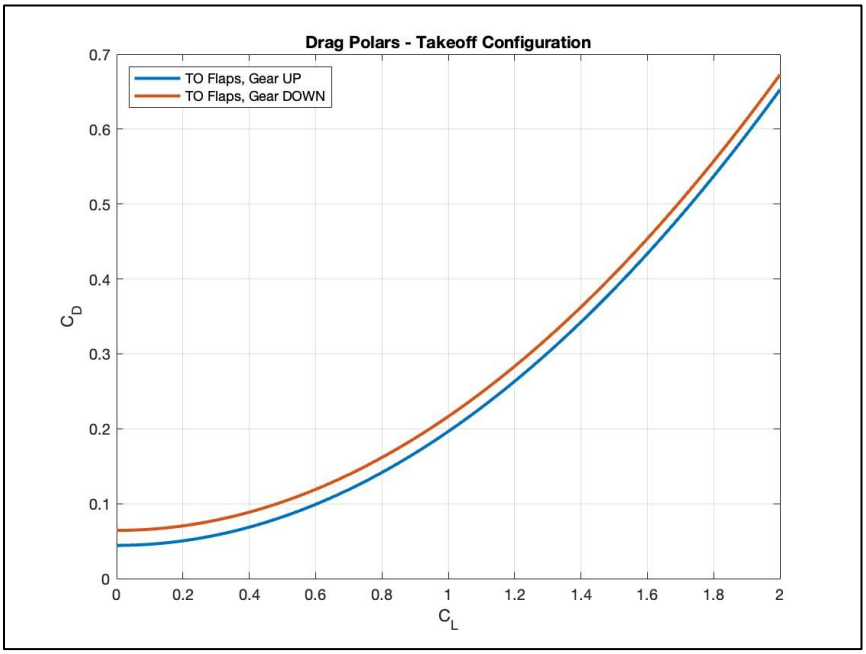

Figure 19: Drag polars for Configuration WTO (Takeoff configuration)

The drag polars developed in this section define the aerodynamic behavior of the aircraft across its full range of mission configurations. The clean configuration establishes the minimum-drag reference condition and captures the

effects of increasing Mach number, while the takeoff and landing configurations illustrate the substantial drag rise associated with elevon deployment and landing gear usage. Since all stores are carried internally, no external drag penalties arise in combat or weapons-carry configurations, resulting in consistent aerodynamic characteristics across those modes. Together, these polars provide a complete representation of the aircraft's drag performance and support all later analyses involving stability, control, and mission performance.

7.8 Moment Coefficients

This section develops the relationship between lift coefficient and pitching-moment coefficient for the carrier-based fighter. The goal is to obtain simple linear curves of C_m versus C_L for the main operating configurations so that trim, stability, and control characteristics can be evaluated consistently with the lift and drag models defined earlier. All curves are referenced to the aircraft center of gravity and are based on the geometry and neutral-point location established in the static-margin analysis. For the clean configuration, the $C_m - C_L$ curve was generated at 100 KTAS, sea-level, 90°F conditions. Using the neutral-point location and center-of-gravity position from the stability spreadsheet, the static margin is approximately five percent, which gives a negative slope of the $C_m - C_L$ line. The clean curve in Figure 13 shows this linear nose-down trend with increasing lift, indicating positive longitudinal static stability. The line is positioned so that the aircraft is trimmed near a moderate lift coefficient representative of one-g level flight at the design gross weight.

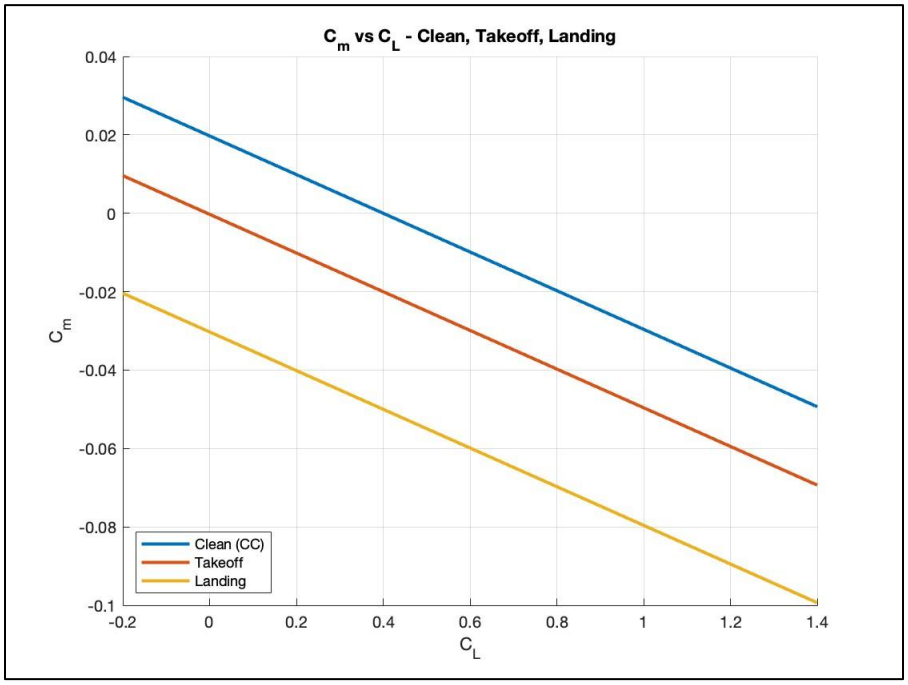

Figure 20: C_m vs C_L for clean-cruise, takeoff, and landing

To obtain the takeoff and landing curves, a build-up approach was used starting at the airfoil level and progressing to the complete airplane. First, two-dimensional airfoil pitching-moment data for the selected wing and tail sections were used to define the basic moment at the quarter-chord. This was converted to a finite-wing contribution using the mean aerodynamic chord and the wing lift-curve slope, with adjustments for the actual twist distribution and wing incidence angle used in the planform design. For cruise, high-g maneuvering, and the various subsonic and supersonic mission segments defined in the SRD, the linear portions of these $C_m - C_L$ curves are used directly. At a given Mach number and configuration, the airplane is assumed to operate within the range where pitching moment varies approximately linearly with lift, so a single slope and intercept fully describe the trim and static-stability behavior. This allows the same moment model to be applied consistently in later performance and control analyses, including cruise trim setting, maneuver load-factor calculations, and evaluation of longitudinal stability across the mission envelope.

7.9 Summary

Table 8 : Summary Values

Wing Planform (ft^2)			662.3			
lean	C_D	=	0.0193	+	0.1429	C_L^2
Takeoff Configuration, Gear UP	C_D	=	0.0443	+	0.1521	C_L^2
Takeoff Configuration, Gear DOWN	C_D	=	0.0643	+	0.1521	C_L^2
Landing Configuration, Gear UP	C_D	=	0.1093	+	0.1626	C_L^2

VIII. Propulsion

8.1 Engine Selection

The F-57 Man o' War employs a twin-engine propulsion system based on the General Electric F110-GE-129 afterburning turbofan. This engine family has a long carrier lineage, having been integrated successfully on U.S. Navy F-14 variants. The F110 architecture has therefore already been proven structurally and mechanically compatible with high sink-rate carrier landings, deck operations, and the associated corrosion and a high FOD environment, making it an ideal low-risk choice for a new carrier-based strike aircraft. In addition, the F110 enjoys a mature global support ecosystem, the engine is in widespread service on multiple fighter platforms, which translates into established mechanical infrastructure, a deep spare-parts pipeline, and existing maintenance procedures and training. This large installed base is expected to reduce life-cycle costs and shorten turnaround times for repairs and overhauls relative to more niche or developmental engines. The selected configuration assumes a unit flyaway cost of approximately $7 million per engine, which keeps propulsion acquisition costs in line with the overall life-cycle cost targets for the F-57.

From a performance standpoint, the F110-GE-129 provides 29,000 lbf maximum thrust in afterburner and 17,500 lbf in military power, giving an engine thrust-to-weight ratio of about 7.3:1 in afterburner and 4.3:1 in military power. In a twin-engine installation this yields 58,000 lbf total maximum thrust, which, when combined with the projected takeoff gross weight of the F-57, provides adequate thrust margins for catapult launch, high-subsonic cruise, and the required dash segments, as demonstrated in the takeoff and mission performance analyses in Section 9. The engine's physical dimensions (approximately 182 in length and 46.5 in diameter) are compatible with the F-57's blended-body flying-wing fuselage, allowing efficient inlet and nozzle integration without excessive penalty in wetted area or volume allocation. Finally, the F110's sea-level mass flow of roughly 270 lb/s provides a strong basis for inlet sizing and ensures desired thrust in hot-day, sea-level carrier conditions. Overall, the F110-GE-129 offers a well-balanced combination of proven carrier suitability, logistics maturity, acquisition cost, and high specific thrust, making it the most suitable propulsion choice for the F-57 Man o' War. As seen in OEI analysis even one engine is more than enough with afterburner to clear both the flight deck and an airfield.

8.2 Inlet Sizing

The inlet sizing begins with the airflow requirement of the F110-GE-129 engines. Each engine draws approximately 270 lb/s of air, and since the aircraft uses one inlet per engine, the sizing is performed individually for each inlet. The design condition chosen for inlet sizing is super cruise at 35,000 ft and Mach 1.6, which represents the primary high-speed cruise regime for the aircraft. At this altitude, the atmospheric speed of sound is approximately 968 ft/s, which allows the freestream velocity to be computed directly from the Mach number.

$$V_\infty = M_\infty a_\infty = 1.6 \times 968 = 1549 \text{ ft/s}$$

To determine the required inlet capture area, mass continuity is applied at the capture plane ahead of the inlet. The required mass flow, freestream density, velocity, and an assumed capture efficiency of 0.95 are used in the continuity equation. This relationship defines how much geometric inlet area is required to ingest the necessary mass flow at the design condition.

$$\dot{m} = \rho_\infty V_\infty A_{\text{cap}} \eta_{\text{cap}}$$

Solving for the capture area gives the following expression:

$$A_{\text{cap}} = \frac{\dot{m}}{\rho_\infty V_\infty \eta_{\text{cap}}}$$

Using the density at 35,000 ft (0.000736 slug/ft³), the freestream velocity from above, and the 270 lb/s engine mass flow, the required capture area becomes:

$$A_{\text{cap}} = \frac{270}{(0.000736)(1549)(0.95)} = 7.71 \text{ ft}^2$$

The actual geometric inlet area from the aircraft's planform design is 1103.79 in² per inlet. Converting this into square feet yields:

$$A_{\text{intake}} = \frac{1103.79}{144} = 7.67 \text{ ft}^2$$

This value is almost identical to the required 7.71 ft², differing by less than half a percent. This indicates that the designed inlet geometry is extremely well-matched to the engine mass-flow requirement at the chosen super cruise design point. Although the aircraft can reach 50,000 ft and Mach 2, the inlet is not sized for that condition because engines demand substantially less corrected mass flow at such altitudes. Still, evaluating the same inlet area at that high-altitude dash point provides useful context. Using the density at 50,000 ft and the corresponding freestream velocity of 1936 ft/s, the available mass flow becomes:

$$\dot{m}_{50k,M2} = (0.000363)(1936)(7.67)(0.95) = 170 \text{ lb/s}$$

This reduced mass flow at 50,000 ft and Mach 2 is entirely expected and aligns with typical high-altitude engine operating behavior. Finally, the designed inlet area can be summarized as:

$$A_{\text{intake}} = 1103.79 \text{ in}^2 = 7.67 \text{ ft}^2$$

The inlet sizing analysis confirms that the designed inlets meet the airflow requirements of the F110–GE–129 engines with exceptional accuracy at the selected super cruise design condition of 35,000 ft and Mach 1.6. The theoretical capture area needed to ingest the required 270 lb/s per engine is 7.71 ft², while the actual inlet geometry provides 7.67 ft², a difference of less than 0.5%. This near-perfect agreement demonstrates that the inlet design effectively balances aerodynamic efficiency and engine performance without requiring additional enlargement or geometric modification. Furthermore, evaluating the inlet performance at the off-design high-altitude dash condition of 50,000 ft and Mach 2 shows that the inlets continue to supply appropriate mass flow consistently with reduced engine demand at extreme altitude. Overall, the inlet configuration is well-matched to the aircraft's propulsion system and supports both its sustained super cruise capability and its maximum-speed operational envelope.

8.3 Propulsive Integration Design

TBD

8.4 Performance Data

The RCR requests installed performance data in both graphical and tabular form, however for the selected engine a full installed performance deck was not available with a credible source. This report presents the available standard day thrust rating data.

Table 9: F110-GE-129 Performance Metrics

Category	Parameter	Value/Description	Notes/Condition
Thrust	Thrust Class	29,000 lbf	Sea-level static, uninstalled, max AB
Thrust	Military (MIL) thrust	17,000 lbf	Sea level static, no AB
Mass flow	Airflow	270lb/s	Sea-level STD.
Pressure ratio	Overall pressure ratio	30.7:1	At maximum power
Bypass	Bypass ratio	0.76:1	At Maximum power
Weight	Dry weight	3,980 lb	Engine only, no fan case
Geometry	Length/ Maximum Diameter	181.9 in/46.5 in	Engine/Fan case external diameter
Thrust to weight	Max AB	7.3:1	From thrust & dry weight above
Thrust to weight	MIL thrust	4.3:1	From thrust & dry weight above

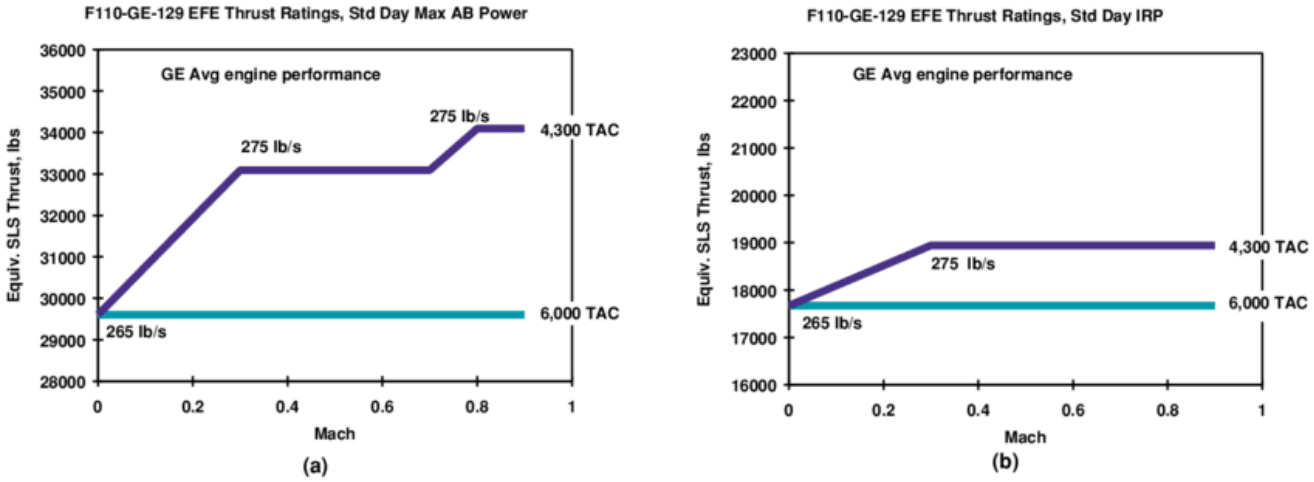

Figure 21: F110-GE-129 Thrust to Mach.

The F110-GE is a low-bypass afterburning turbofan in the 29,000-pound thrust class, providing approximately 17,000 lbf military thrust and 29,000 lbf in maximum afterburning thrust at sea-level static conditions. Its airflow rate is 270 lb/s which is large for an engine of its thrust class, and indicates a core and fan sized to process a lot of air, which directly supports strong thrust production at low altitude where their aircraft will be launching from. The overall pressure ratio of 30.7:1 also relates to high performing turbofan engines because a higher-pressure ratio increases cycle efficiency and allows the engine to generate high specific thrust at the expense of higher turbine temperatures and greater material demands, though with engine core upgrades this will decrease the issue greatly. Finally, the bypass ratio of 0.76:1 is in the low bypass region used for combat aircraft. Lower bypass engines produce some propulsive efficiency for higher specific thrust and ability to use afterburner effectively. Transport engines use higher bypass ratios around 5-10:1 to minimize fuel burning. Together with the thrust-to-weight ratios of 4.3:1 MIL thrust and 7.3:1 AB these parameters confirm that the F110-GE-129 is optimized for high thrust, strong acceleration, and maneuvering performance rather than TSFC. This makes it perfect for the F-57 Man o' War's role as a carrier-based strike and air-defense aircraft, where the team needed short-field performance like high-speed dashes and combat.

Figure 21 above shows the manufacturer's equivalent sea-level thrust ratings for the F110-GE-129 as a function of Mach number for both maximum afterburner power and intermediate rated power. In both plots lower turquoise line represents a constant sea level thrust for a more conservative 6,000 Total Accumulated Cycles (TAC). Which is a usage/life metric used for scheduling maintenance intervals. The rise from Mach 0 to 0.3 shows an increase in inlet pressure which relates to more thrust, this flows into the flat sections meaning the engine has reached a limit set by the manufacturers limiting the internal temperature and thrust. The small step up near higher Mach in plot (a) reflects another operating regime that allows the aircraft to squeeze more thrust while still maintaining manufacturers rating, though this level should not be held for much time due to internal temperatures. It is important to keep in mind that this data is presented in equivalent SLS thrust and no additional installation loss corrections are applied.

IX. Performance

9.1 Takeoff Analysis

There are 4 main criteria for taking off from the CVN-68 and CVN-78 class carriers. The first being that their aircraft must not sink less than 10ft at the end of the power stroke, to which the team calculated minimum velocities of 99.43 and 97.33 knots for strike and air to air, respectively. The second requirement is that their minimum end airspeed must be supported at 90% of their max lift coefficient –the team calculated it to be 123.20 and 121.38 knots. Third, the team must ensure their aircraft remain accelerated at a minimum of 0.065g, where g is the gravitational acceleration: the team found this to be 75.66 and 73.82 knots. Lastly, what the team found to be their main governing speed is their minimum aircraft control speed with one inoperative engine. Seeing as the team are a naval jet, two engines are highly necessary to minimize any failures, which makes these criteria extremely important. Unfortunately, the team found that the air speed required of their aircraft is 140.26 knots for their strike payload and 138.7 for their air to air, which means this requirement is unsatisfied as noted in the system requirements on line 12. The catapult, based on their dead and takeoff weight, will provide their aircraft with 135 knots, which the team were able to find using the catapult curve in figure 55. The aircraft fall 5.26 knots short on their strike payload, and 3.7 knots on their air-to-air payload. The main consideration to rectify this would be to alter their weight, and make it lighter, due to the surface area of their wings at this stage being relatively finalized, and the team cannot increase their max lift coefficient any more than it is. However, as the team looked more into their aircraft, the team may find there is room to resize and alter the wings and weight of the aircraft.

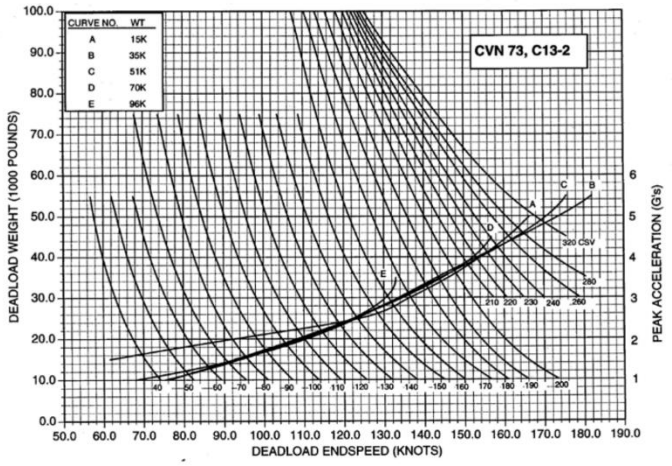

Figure 22: Minimum Performance and Load Factor Curves

Table 10: Takeoff Velocity Profiles

	Air to Air	Strike
90% C_L	121.83	123.20
Sink ≤ 10ft	97.33	99.43
Longitudinal Acc ≥ 1.2398 knots	73.82	75.66
Min Control Airspeed OEI	138.7	140.26
Governing Airspeed	138.7	140.26

9.2 Landing Analysis

As a carrier-based aircraft, the F-57 will perform arrested landings on both CVN-68 and CVN-78 class aircraft carriers. Both the Nimitz and Gerald R. Ford class carriers utilize cable assisted recoveries and these landings can be analyzed for both their Air to Air and Strike loadouts.

For the approach weight, several weight requirements are assumed. These include enough fuel for 20 minute loiter (10,000 ft) and two landing attempts, 25% of the max fuel weight and 50% of the payload still on board. The previous

weight requirements added to the Operating Empty Weight of 29,600 lbs enable calculations of aircraft weight at recovery for both loadouts.

As per the RFP, an assumed temperature of 89.8°F at sea level, thus air density is to be 0.002237 $\frac{slugs}{ft^3}$. On landing stall velocity will be directly affected by landing weights and the assumed C_{L_max}. The calculated stall velocities could be inferred as being too low for such aircraft, however, having chosen a $C_{L\_max} = 2$, it is assumed that elevons are symmetrically deployed for additional lift augmentation, as well as making use of high angles of attack for vortex lift generation.

$$V_{stall_L} = \sqrt{\frac{2W}{\rho S C_{L_{max}}}}$$

Moving onto approach velocity, it is to be greater than 10% above stall speed yet less than 145 knots. For the F-57, it shall approach at 30% greater than V_{stall_L} to ensure sufficient control and maneuverability. Finally, it is assumed that its arrestment engaging speed is 5% greater than approach speed. The arresting gear performance chart helps estimate the aircraft's hook load when in contact with the cable upon touchdown. The finalized calculations with these various assumptions are displayed below.

Table 11: Recovery Performance

	Air to Air	**Strike**
$W_{approach}$ (lbs)	37807	39042
$V_{stall\_landing}$ (knots)	95.77	97.32
$V_{approach}$ (knots)	123.03	125.02
$V_{engaging}$ (knots)	129.18	131.26
Hookload (lbs)	131,000	138,000

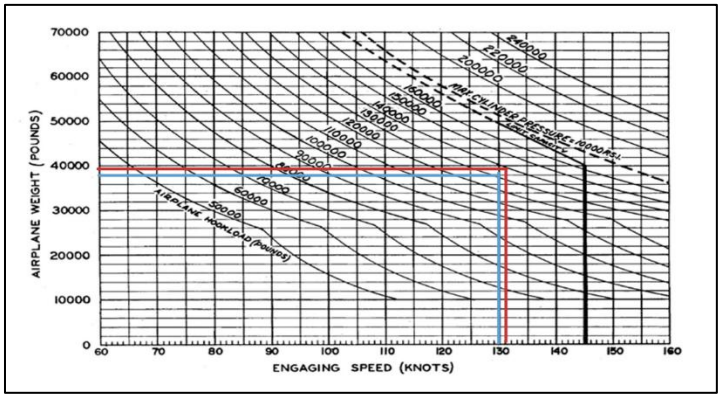

Figure 23: Arresting Gear Performance Curves

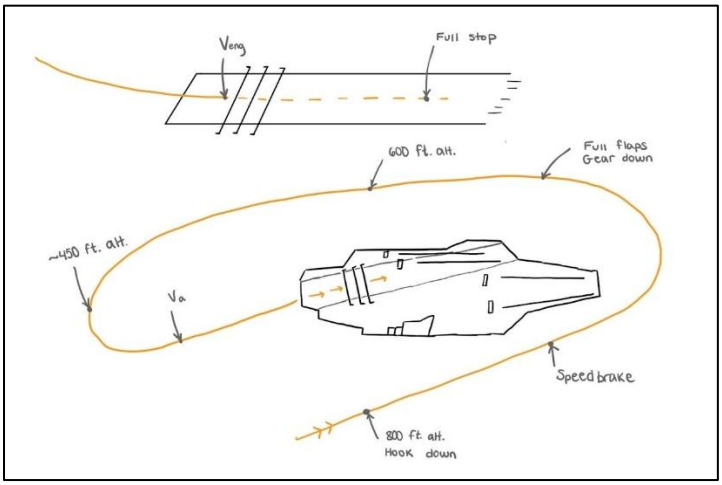

Figure 24: Carrier Landing Pattern

9.3 One Engine Inoperative

Table 12: One Engine Inoperative Table

Rate of Climb OEI Requirement (Feet per minute)	200
Density (Sea Level) ($\frac{slug}{ft^3}$)	0.002378
Temperature (°F)	89.8
Air Density Ratio	0.944
Weight and Surface Ratio @ Take Off (PSF)	80
Calculated Velocity (FPS)	360.55
Calculated Velocity (Knots)	213.5
Take Off Requirement Climb (Knots)	140.6

In Table 12 the defined the velocity for the aircraft's rate of climb while experiencing a one engine inoperable configuration as 200 feet per minute. Under their current configuration at sea level with an approximate density at 0.0024 $\frac{slugs}{ft^3}$ and a temperature of about 89.8 °F. The team found the ratio between the aircraft weight and surface area at takeoff configuration to be about 80 PSF. Taking this value into account, relating the air density ratio of about 0.94, and all information regarding the coefficient of drag and lift located in section 7the team find that the calculated velocity is about 360.55 FPS or approximately 213.5 knots. Referring to section 9.1, the team take that the governing speed for takeoff is about 140.6 knots. Therefore, with the calculated value this proves that with its current configuration the team can achieve the rate of climb documented in the requirement above. Refer to the steps below in calculating the valued presented.

$$\left(\frac{W}{S}\right)_{TO} = \left(\frac{60966}{645.7}\right) = 80$$

$$V = \sqrt{\frac{2*\left(\frac{W}{S}\right)_{TO}}{\rho*\sqrt{C_D*\pi*(AR)*e}}} = \sqrt{\frac{2*80}{0.002377*\sqrt{0.0443*\pi*2.4*0.8}}} = 360.55 \text{ fps}$$

9.4 Loss and Brake Analysis

For carrier operations, there is no meaningful "Loss and Brake" (LAB) launch after launch commit, once the catapult stroke begins the aircraft is forced off the deck and cannot reject the takeoff. Therefore, the only relevant case is the "Loss and Continue" (LAC) option. To determine whether their aircraft can still take off after the power stroke we'd have to assess the thrust and drag for OEI. Thrust with the afterburner of their F110-GE-129 engine provides 29,000 lbs of force. Calculating drag the team can use equations given in Pamadi and the velocity to satisfy the minimum requirement in Section 2.3 shown above the team also considers that control-surfaces are extended and gear still down. Solving for drag the team get a force of 14340.1 lb. With these values the team have T - D = 29,000lb - 14340.1 lb = +14659.9 lb of excess thrust, meaning with OEI their aircraft can still take off with a T/D of 2.02 their aircraft provide twice the drag load with only one engine. After takeoff their climb gradient would be T - DW which turns out to be 0.2156 -> 21.56% making their worst-case OEI scenario more than survivable

Though the team can't ignore that their aircraft will take off from a normal airstrip. The OEI conditions are as follows: 5000 ft runway, No wind, 89.8˚F, low velocity engine failure. Balanced field length (BFL) is the runway distance for which the accelerate and go and accelerate and stop distances are equal in the critical one engine inoperative (OEI) case. In the accelerate and go case, the aircraft loses an engine at the engine failure speed V_{EF}, continues the takeoff on the remaining engine, and reaches the obstacle clearance speed V_{obs} by the end of the runway. In the acceleration and stop case, the aircraft accelerates from rest to the decision speed V_1, the crew rejects the takeoff at V_1, and the aircraft brakes to a full stop by the end of the runway. When the field is balanced, both options use essentially the same runway distance. For the F-57 Man o' War, the team assumed a design balanced field length (S_{BFL}) of 3640 ft.

The analysis starts with the stall speed in takeoff configuration, Vs = 197.27 ft/s. The speed schedule is then defined with fixed ratios:

$$V_1 = 1.05 \times V_s \text{(decision speed)}$$

$$V_R = 1.10 \times V_s \text{(rotation speed)}$$

$$V_{TO} = 1.15 \times V_s \text{(Takeoff speed)}$$

$$V_{obs} = 1.30 \times V_s \text{(Speed at obstacle)}$$

$$V_{EF} = 0.80 \times V_1 \text{ (engine failure speed)}$$

Table 12: Field Velocities

Velocity Name	Velocity (KTAS)
Engine Failure (EF)	98.18
Decision (1)	122.72
Rotation (R)	128.57
Takeoff	134.41
Obstacle	151.94

To model the accelerate-go path, the team assume a constant takeoff acceleration that carries the aircraft from break release to V_{obs} at the balanced field length distance.

$$V^2 = 2\,a\,s \rightarrow s(V) = \frac{V^2}{2\,a}$$

The effective acceleration is

$$a = \frac{{V_{obs}}^2}{(2 \cdot s_{BFL})}$$

With this acceleration, the distance to reach any speed V on the go path is:

$$s(V) = \frac{V^2}{2\,a}$$

For the F-57 this yields, for example, S_{EF}(distance to V_{EF}), sV_1 (distance to V_1), sV_R (distance to V_R), and s_{TO} (distance to V_{TO}). Numerically, the engine failure speed V_{EF} is reached at about 1520 ft, the decision speed V_1 at about 2375 ft, rotation at about 2600 ft, liftoff at about 2850 ft, and V_{obs} at the full 3640 ft. The go path velocity as a function of distance is then:

$$V_{go}(s) = \sqrt{2 \times a_{go} \times s}$$

For the acceleration and stop case, the aircraft first accelerates from rest to $V_1$with the same ago, then brakes from V_1 back to zero with a constant deceleration chosen so that the total distance equals the same BFL. The distance to accelerate to $V_1$is:

$$sV_1 = \frac{{V_1}^2}{2\,a_{go}}$$

The braking distance from V_1 to stop with constant deceleration a_{brake} is:

$$s_{brake} = \frac{{V_1}^2}{2\,a_{brake}}$$

Balanced field require:

$$s_{BFL} = sV_1 + s_{brake}$$

Solving for a_{brake} gives:

$$a_{brake} = \frac{{V_1}^2}{2 \times (s_{BFL} - sV_1)}$$

For the F-57 this corresponds to a net takeoff acceleration of roughly 0.28 g and an effective braking deceleration of roughly 0.53 g, which are reasonable for a high-performance carrier-based aircraft. The stop path velocity is then defined piecewise as:

$$V_{stop}(s) = \sqrt{2 \times a_{go} \times s} \quad \text{for } 0 \le s \le sV_1 \text{ (accelerating)}$$

$$V_{stop}(s) = \sqrt{{V_1}^2 - 2 \times a_{brake} \times (s - sV_1)} \quad \text{for } s\,sV_1 < s \le s_{BFL} \text{ (braking)}$$

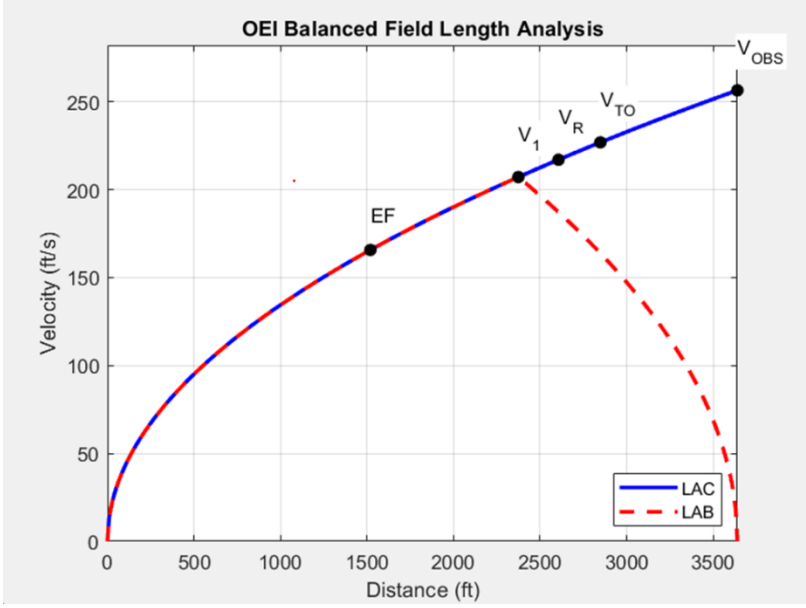

Figure 25: Field Length Analysis

In the resulting distance plot, the "go" curve V_{go} (s) increases from zero and reaches V_{obs} at 3640 ft, while the "stop" curve V_{stop} (s) follows the same acceleration up to sV_1 and then curves back down to zero velocity exactly at 3640 ft. The markers for V_{EF}, V_1, V_R, V_{TO}, and V_{OBS} show where each key speed occurs along the runway. For the F-57 Man o' War, this analysis shows that if an engine fails at about 98 kt the aircraft can continue the takeoff and reach obstacle–clearance speed by 3640 ft, and if the crew elects to reject the takeoff at about 123 kt the aircraft can safely stop in the remaining runway. This demonstrates that the chosen speed schedule and runway length provide a balanced and operationally acceptable takeoff performance for the aircraft.

9.5 Summary

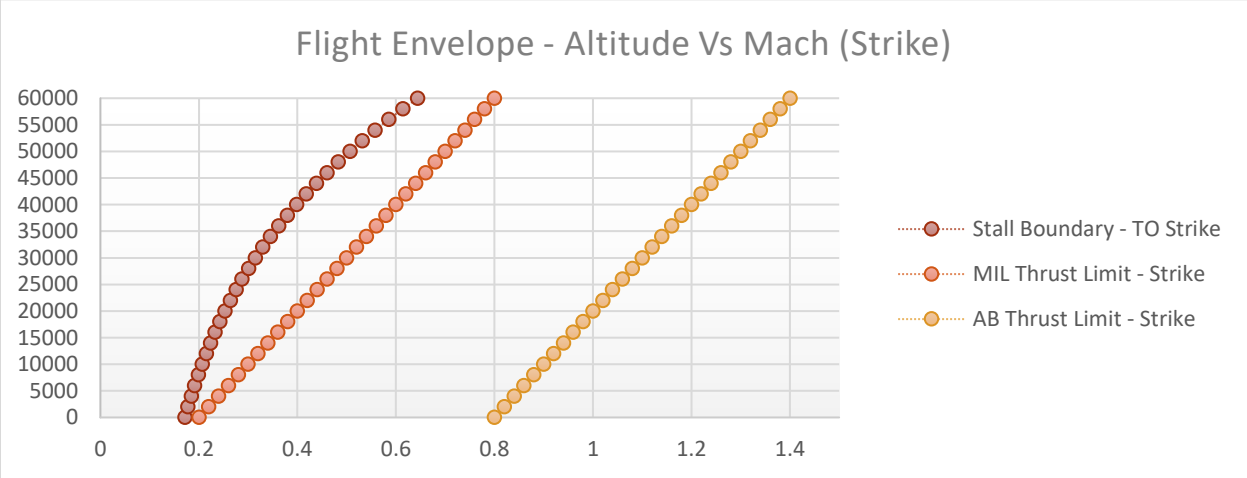

Figure 26: Flight Envelope for Strike

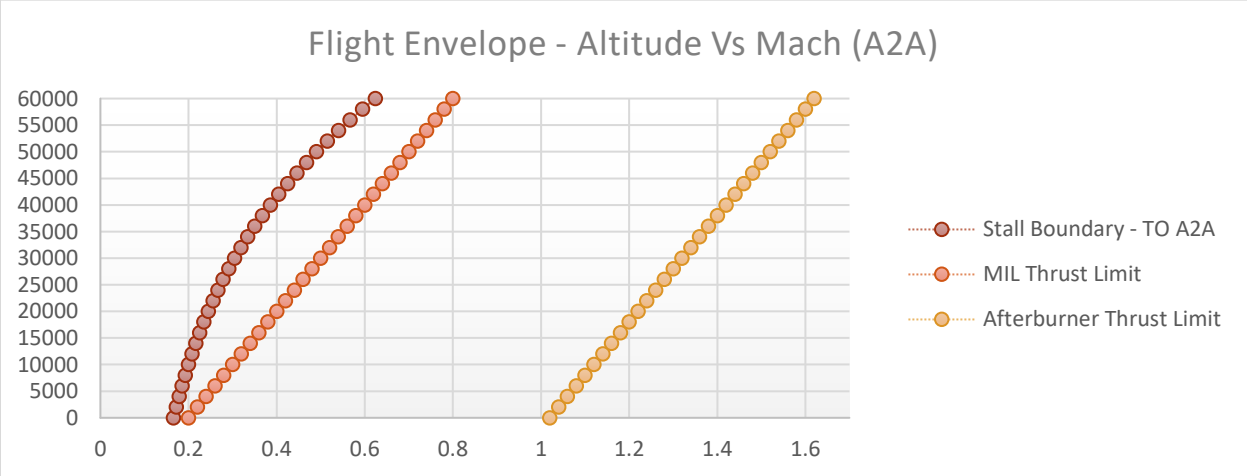

Figure 27: Flight Envelope for Air to Air

Located above are flight envelopes for both the strike and air to air payloads, which represent the most restrictive operational cases, considering both military (MIL) and afterburner (AB) thrust settings. The stall boundaries were determined using the 1-g lift condition, a max lift coefficient of 2, and various altitudes up to 60000m. From the altitude various temperatures and densities were found which led to further derivation that ultimately resulted in the final curves shown above. The furthest curve left on both figures represent the left boundary of the flight envelope defined by the stall Mach number, which increases with altitude due to the decreasing air density. The right boundaries are defined by thrust availability, with the military power envelope collapsing rapidly with altitude. Moving on to the

afterburner thrust limit, it is observable that the achievable Mach range significantly expands, and the area between represents achievable steady, level flight, otherwise known as the buffet boundaries.

Table 13: Performance Requirements Cross-Verification

9	Catapult end-speed (sink/deck run)	≤10 ft sink; ≤32 ft post-stroke deck run
10	Catapult end-speed (lift limit)	≥ speed at 0.9 CLmax (power-off, OGE)
11	Catapult end-speed (acceleration limit)	≥ speed where ax ≥ 0.065 g at γ = 0°
12	Catapult end-speed (control, multi-engine)	≥ minimum control speed with one engine inoperative
13	Arrestment engaging speed	V_engage = 1.05 × V_approach
14	Approach speed limits	>1.10 × V_stall and <145 kt
15	Arrestment landing weight basis	Include fuel for 20 min loiter @10k ft + 2 landing attempts; 25% max fuel wt; 50% store wt

X. Stability and Control

The tailless design of the F-57 Man-O'-War makes heavy usage of advanced next generation fly-by-wire computational control systems. The future of flight is becoming increasingly digital, with geometry still contributing to flight capabilities. With tailless configuration the static margin is only dependent on the wing geometry. The static margin is estimated at 4.93% with a center of gravity at 370 inches. The equation for static margin is equal to the following equation.

$$H_n = \frac{x_n - x_{c.g.}}{\bar{c}}$$

This value means that the airplane is slightly statically stable, which is valid for a fighter aircraft, as too much stability would hinder the aircraft's ability to perform military ready maneuvers. This is comparable mostly to the F-16, which has a suspected static margin of 0-5%. This value also agrees with the philosophy that this aircraft design would require a heavy use case of fly-by-wire technologies as the static margin is very low and would benefit from advanced computational technologies. The horizontally mounted control surfaces, as well as thrust vectoring, will be the sources for roll, pitch, and yaw, authority. The inward control surfaces, the elevons are wide enough for high pitch and roll authority, and the split rudders on the outward portion of the wing, will provide yaw authority. With 18% of the wing surface area being roll and pitch control, and 10% of the wing being yaw control, these sizes are considered effective for controlled and stabilized flight.

XI. Configuration Spreadsheet

TBD

XII. Life Cycle Costs

Table 14: Aircraft Values

Empty Weight (lbs) w/ 60% Fuel	23944.2
Maximum Speed	1069
Cumulative Quantity Produced	500
Sea Level Maximum Thrust (lbf)	58000
Maximum Mach Number	1.6
Turbine Inlet Temperature (Rankine)	3200

Table 15: Total Cost of Production

Airframe Engineering	$27,100,526.84	0.06%
Development Support	$473,064,456.50	0.99%
Flight Test Operation	$33,758,242,461.08	70.61%
Tooling	$15,628,874.42	0.03%

Manufacturing Labor	$433,479,921.20	0.91%
Quality Control	$56,352,389.76	0.12%
Total Cost of Materials	$3,291,990,027.93	6.89%
Engine	$8,661,520.48	0.02%
Avionics	$9,600,000,000.00	20.08%
Operation and Maintenance	$150,000,000.00	0.31%
Total Cost (1993)	$47,814,520,178.20	
Total Cost (2025)	$107,104,525,199.16	
Cost Per Unit	$214,209,050.40	

Table 13 labeled as the aircraft's value defines crucial components that are utilized to calculate the total cost outlined in chapter 24 of Nicolai's text. The text has defined the crucial components as empty weight at 60% fuel, maximum speed, cumulative quantity produced, sea level thrust, maximum Mach number and the turbine inlet temperature in Rankine. Table 14 outlines the final cost for the Man O' War program. The table defines the total cost of production for 500 aircraft as 107 billion dollars. The unit cost per aircraft comes out to be around 214 million dollars. Comparing the unit cost of their aircraft to the F-35C, it currently has a fly away cost of about 108 million, although this price does not include long-term maintenance, spare parts packages, weapons, avionics suites and lifecycle sustainment. The current difference between the F-57 and F-35 has a difference of about 107 million dollars. The team can state that the equation provided by Nicoli considers the subsections that are currently classified due to military access. Looking at table 14 the team can note that the two major components of cost for the F-57 can be attributed to the flight test operation (70.6%) and avionics (20.08%). To reduce the final price for the jetthe teamcan reduce the amount of Flight Test Operations and or the avionics suite within the jet. At the current level of the F-57the teamhave state-of-the-art avionics suites that are utilizing swarm technology that has been proposed by Northrop Gunman. Refer below the calculations provided by Nicolai to obtain values in table 14.

Airframe engineering: $E = 4.86 * W^{0.777} S^{0.894} * Q^{0.163}$

Development support cost: $D = 66 * W^{0.63} * S^{1.3}$

Flight Test Operations: $F = 1852 * W^{0.325} S^{0.822} Q_D^{1.21}$

Tooling: $T = 5.99 * W^{0.777} * S^{0.696} * Q^{0.263}$

Manufacturing Labor: $L = 7.37 * W^{0.82} * S^{0.484} * Q^{0.641}$

Quality Control: $QC = 0.13 * L$

Total Cost of Materials: $M = 16.39 * W^{0.921} * S^{0.621} * Q^{0.799}$

Engine: $P = 2306\ [0.043_{TSLS} + 243.3_{Mmax} + 0.969 * T_R - 2228]$

Acknowledgments

The team would like to recognize the entire Aerospace Engineering department for contributing to the team academic career. Without the guidance and instruction of the faculty the team would not be able to have achieved their first version of their senior design capstone project. The team would like to formally thank Geoffery Butler for his time and dedication to the Aerospace Engineering class of 2026. Without Professor Butlers guidance the current teams taking AE 460A would not have clear guidance from industry standards.

References

[1] F/A-18E/F Super Hornet Image. Military.com. Accessed Dec. 14, 2025. https://images01.military.com/sites/default/files/media/equipment/military-aircraft/fa-18e-f-super-hornet/2014/02/fa-18e-f_001.jpg.

[2] F-35 Carrier Squadron Air Wing Image. The War Zone. Accessed Dec. 14, 2025. https://www.twz.com/wp-content/uploads/images-by-url-twz/content/2022/02/F35-Carrier-Squadron-Air-Wing.jpg?quality=85.

[3] Hornet Landing Gear Image. The Lexicans. Accessed Dec. 14, 2025. https://thelexicans.wordpress.com/wp-content/uploads/2017/06/hornetgear.jpg?w=584.

[4] NACA 64(2)-06 Airfoil Details. Airfoil Tools. Accessed Dec. 14, 2025. http://airfoiltools.com/airfoil/details?airfoil=naca64206-il.

[5] F110-GE-129 EFE Average Thrust Ratings on a Standard Day. ResearchGate. Accessed Dec. 14, 2025. https://www.researchgate.net/figure/F110-GE-129-EFE-Average-Thrust-Ratings-on-a-Standard-Day-a-Max-A-B-Power-and-b_fig2_267483234.

[6] F110-GE-129 Engine Datasheet. GE Aerospace. Accessed Dec. 14, 2025. https://www.geaerospace.com/sites/default/files/datasheet-F110-GE-129.pdf.

[7] Lorenz III, P. "Longest-running jet engine test at AEDC is complete." Arnold Air Force Base, Nov. 22, 2010. Accessed Dec. 14, 2025. https://www.arnold.af.mil/News/Article-Display/Article/409489/longest-running-jet-engine-test-at-aedc-is-complete/.